

AMSbench: A Comprehensive Benchmark for Evaluating MLLM Capabilities in AMS Circuits

Yichen Shi^{*1,4}, Ze Zhang^{*4}, Hongyang Wang^{*4}, Zhuofu Tao², Zhongyi Li⁴
Bingyu Chen², Yaxin Wang², Zhiping Yu³, Ting-Jung Lin^{†4}, Lei He^{†2,4}

¹ Shanghai Jiao Tong University ²University of California, Los Angeles

³Tsinghua University ⁴Eastern Institute of Technology, Ningbo

{tlin@idt.eitech.edu.cn} {lhe@ee.ucla.edu}

Abstract

Analog/Mixed-Signal (AMS) circuits play a critical role in the integrated circuit (IC) industry. However, automating Analog/Mixed-Signal (AMS) circuit design has remained a longstanding challenge due to its difficulty and complexity. Recent advances in Multi-modal Large Language Models (MLLMs) offer promising potential for supporting AMS circuit analysis and design. However, current research typically evaluates MLLMs on isolated tasks within the domain, lacking a comprehensive benchmark that systematically assesses model capabilities across diverse AMS-related challenges. To address this gap, we introduce AMSbench, a benchmark suite designed to evaluate MLLM performance across critical tasks including circuit schematic perception, circuit analysis, and circuit design. AMSbench comprises approximately 8000 test questions spanning multiple difficulty levels and assesses eight prominent models, encompassing both open-source and proprietary solutions such as Qwen 2.5-VL and Gemini 2.5 Pro. Our evaluation highlights significant limitations in current MLLMs, particularly in complex multi-modal reasoning and sophisticated circuit design tasks. These results underscore the necessity of advancing MLLMs’ understanding and effective application of circuit-specific knowledge, thereby narrowing the existing performance gap relative to human expertise and moving toward fully automated AMS circuit design workflows. Our data is released at this URL.

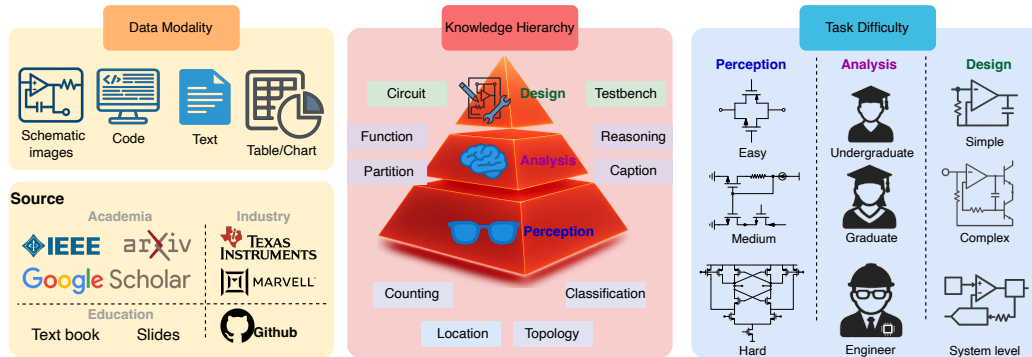


Figure 1: **Overview of AMSbench.** AMSbench includes multimodal question-answer pairs collected from both academia and industry. The tasks are divided into schematic perception, circuit analysis, and circuit design.

1 Introduction

The rapid advancement of large language models (LLMs) and multimodal large language models (MLLMs) has led to significant breakthroughs across diverse domains, including autonomous driving [1], scientific research [2, 3], mathematics [4, 5, 6], and programming [7]. In the domain of Electronic Design Automation (EDA), these models have shown promise, particularly in the automated design of digital circuits [8]. On the contrary, automating analog/mixed-signal (AMS) circuit design has been a longstanding challenge for its reliance on human experience. Today’s AI-driven automatic AMS design still faces considerable challenges due to the scarcity of high-quality data and the intrinsic complexity of multi-modal data. As a result, the exploration and application of LLMs in AMS circuit design remain limited and exhibit relatively poor performance [9, 10, 11]. Furthermore, current applications focus on verbal information, while AMS circuits rely on other modalities as well, such as schematics, plots, and charts.

A primary obstacle lies in the limited capability of existing MLLMs to accurately interpret circuit schematics. Unlike netlists, schematics convey richer and more nuanced structural information beyond abstract connectivity. Recent work [12, 8] has recognized this limitation and introduced tools capable of automatically converting schematics into netlists, thereby enabling the creation of large-scale, high-quality datasets suitable for training models. With the recent advancements in the visual capabilities of MLLMs—such as GPT-4o [13] and Qwen2.5 [14]—schematic recognition accuracy has improved significantly, laying a solid foundation for the automated analysis and design of AMS circuits. Despite these advancements, current applications often focus on isolated tasks—such as netlist generation [10, 15] and error identification [16]—while lacking comprehensive evaluation frameworks.

In particular, there has been little systematic investigation into the following three fundamental questions:

1. How accurately can models recognize and interpret AMS circuit schematics?
2. What is the upper bound of domain-specific knowledge that models can attain in AMS circuit analysis and design?
3. To what degree are models capable of supporting the automation of AMS circuit design?

To address these questions and bridge the existing research gaps, we propose AMSbench, a comprehensive benchmark designed to evaluate the capabilities of advanced models in the context of AMS circuit design. AMSbench assesses model performance across three key dimensions: **perception**, **analysis**, and **design**.

In the perception task, the objective is to evaluate how accurately MLLMs can generate netlists directly from circuit schematics, reflecting their schematic recognition capabilities. This is a non-trivial challenge due to the large number of components and their intricate interconnections. We further decompose this task into sub-tasks such as component counting, component classification, and interconnect recognition, culminating in the primary goal of accurate netlist generation. The analysis task examines the models’ understanding of circuit functionality, ability to identify critical building blocks, and comprehension of trade-offs among performance metrics—key aspects in AMS circuit design and verification. Finally, the design task investigates whether models can synthesize circuits that satisfy given specifications. We also evaluate their ability to generate appropriate testbenches to assess circuit performance across multiple criteria.

To the best of our knowledge, AMSbench is the first holistic benchmark that systematically evaluates the performance of advanced models in AMS circuits. The overall benchmarking results of state-of-the-art models using AMSbench are illustrated in Fig. 2. Our contributions are summarized as follows:

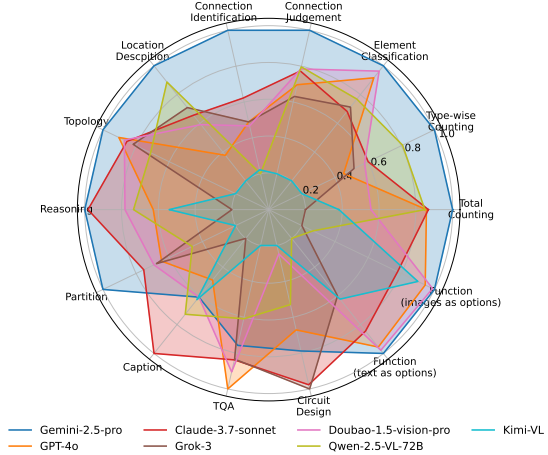


Figure 2: Comparison of top MLLMs on 14 sub-tasks(w/o DeepSeek-R1 on VQA tasks, which lacks visual processing capability)

- We introduce **AMSbench**, a multimodal benchmark designed to rigorously evaluate the perception, analysis, and design capabilities of MLLMs in the AMS circuit domain. AMSbench consists of three major components: AMS-Perception (6k), AMS-Analysis (2k), and AMS-Design (68).
- We conduct a comprehensive evaluation of both open-source and proprietary models on AMSbench, providing detailed comparisons and performance insights across all tasks.
- We release the AMSbench dataset at the provided URL, fostering transparency and reproducibility in this emerging research area.

2 Related Work

2.1 LLM for circuit design

LLMs have demonstrated remarkable potential in the field of EDA, excelling in tasks related to system-level design [17], RTL [18, 19], synthesis and physical design of digital circuits. This success is primarily due to the modular nature of digital circuit descriptions, which resemble software languages. However, AMS circuit designs, with their transistor-level descriptions, pose a significantly greater challenge for LLMs in terms of accurate understanding and description. Some exploratory work has been undertaken in AMS circuit design [20, 21]. Artisan [11] develops a LLM that automatically generates operational amplifiers by combining advanced prompt engineering techniques like Supervised Fine-Tuning (SFT) and Tree of Thought. Analogcoder [10] proposes using LLMs with predefined sub-circuit libraries to achieve an iterative design and optimization flow. AnalogGenie [9] converts circuit topologies into Eulerian circuit representations and uses SFT for synthesizing circuits based on the design requirements. To ensure that the generated circuits can meet specifications, AnalogGenie applies Reinforcement Learning with Human Feedback (RLHF) [22] as a post-training technique. ADO-LLM [23] combines LLMs with Bayesian optimization to generate higher-quality candidate design samples, enhancing efficiency in the transistor sizing process. Layout Copilot uses multiple intelligent agents to improve the efficiency and performance of automated layout generation. AMSnet-KG [24] employs a knowledge graph-based RAG (Retrieval-Augmented Generation) approach, based on a large-scale, pre-constructed circuit database, to select and generate circuit topologies that meet specifications. However, it is worth noting that these studies mainly focus on purely language-based LLMs, while circuit design often relies heavily on schematic diagrams. Both CHAI [8] and AMSnet [12] have pointed out that existing MLLMs still lack the capability to effectively recognize circuit schematics.

2.2 Benchmarking for EDA

The academic infrastructure for LLM research in EDA has made significant progress. Abundant available benchmarks and datasets have facilitated effective development of LLMs in EDA. VerilogEval [25] and RTLLM [26] introduce benchmarks for evaluating RTL code generation. However, these benchmarks focus primarily on digital circuits. Due to the complexity and irregularity of analog circuits, AMS circuit design is highly experience-driven, making it difficult to establish fair evaluation methods. Hence, benchmarks in the analog circuit domain remain scarce. Analogcoder [10] proposes a benchmark to evaluate LLMs in AMS circuit design, categorizing circuits into three levels: easy, medium, and hard. However, it is limited to the main circuits and did not touch any testbench. [27] presents a benchmark to assess LLMs’ understanding of AMS circuits, including 510 simple questions. Currently, benchmarks in the AMS circuit and EDA domains are limited to verbal questions. However, AMS circuit design is naturally multi-modal, as designers are required to recognize, understand, and reason about circuit schematics.

3 AMSbench Construction

3.1 Data Collection and Curation

To cover a wide range of knowledge and typical question types in the AMS circuit domain, we gather a diverse collection of research papers, textbooks [28, 29, 30, 31], and commercial circuit datasheets. We convert all documents from PDF to Markdown format using MinerU[32], enabling efficient extraction of embedded visual elements such as circuit schematics. For schematic-to-netlist translation,

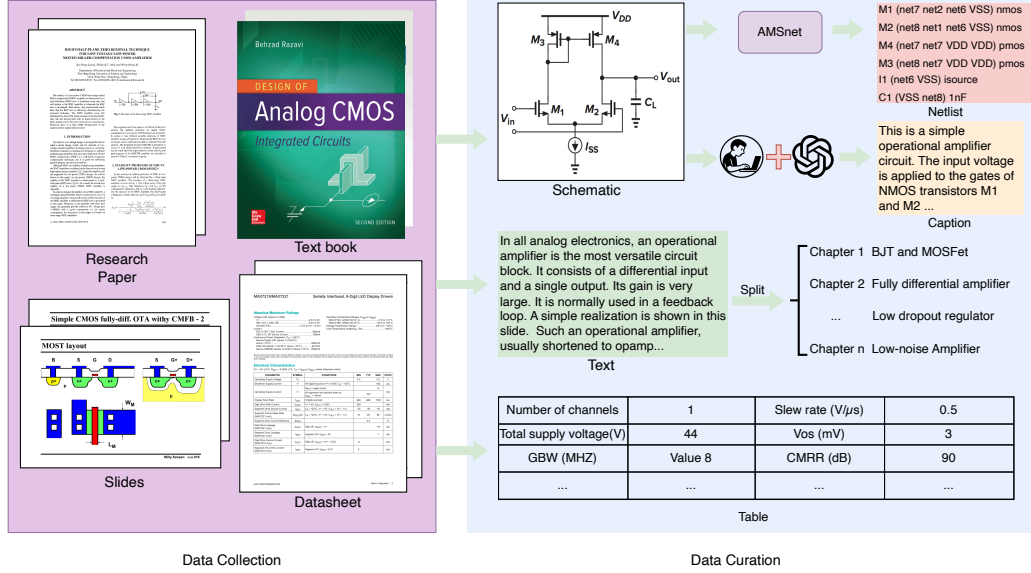


Figure 3: Data collection and curation for AMSbench

we utilize AMSnet[12], which allows us to accurately recover component-level connectivity and circuit topology. To enrich the dataset with semantic information, we use a combination of manual annotations from field experts and outputs from state-of-the-art MLLMs [13, 14]. We then apply carefully crafted prompt engineering and filter strategies to generate detailed schematic captions. This process yields high-quality pairs of <circuit schematic, caption>.

For textbook-derived data, we organize content according to the logical structure and chapter alignment of each source. For datasheet content, we extract structured performance specifications associated with each circuit. Based on the extracted information, we manually construct a question–answer dataset focused on circuit principles, behavior, and performance metrics, as illustrated in Fig. 3.

3.2 Evaluation

The goal of AMSbench is to thoroughly evaluate MLLMs on the potential applications and tasks in the AMS circuit domain, as shown in Fig. 1. For the design of specific problems, we develop a multi-dimensional evaluation framework that includes **perception**, **analysis**, and **design**. This framework addresses the potential uses of MLLMs in assisting users with interpreting and designing circuit schematics, both automatically and semi-automatically. Considering the complex data modalities and diversity within the AMS circuit domain, the tasks encompass Visual Question Answering (VQA) and Textual Question Answering (TQA). These include multiple-choice questions, computational problems, and open-ended generative questions. We systematically construct questions for each task at multiple levels to accommodate various difficulties and circuit types.

Evaluation Dimensions For the **perception** tasks, we focus on recognizing *elements* in circuit schematics. We define an element as any component or device represented by a line in a netlist, such as transistors, resistors, subcircuit symbols, etc. MLLMs are evaluated based on three key aspects:

1. Accuracy in Element Counting: This measures how well the model can identify and count the number of different elements in a schematic. We use tasks *type-wise counting* and *element classification*.
2. Precision in Identifying Connectivity: This assesses the model’s ability to accurately determine how elements are connected to each other. We use tasks *connection judgment* and *connection identification*, where connection judgment uses true-false questions to decide whether two elements are connected, and connection identification requires the model to state connecting elements.

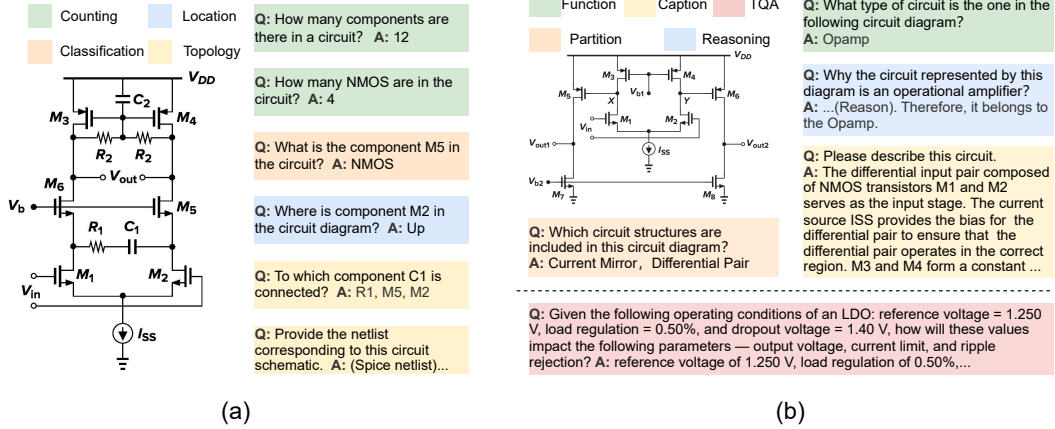


Figure 4: Example of question generation for AMSbench

3. Capability to Recognize the Entire Netlist: This evaluates whether the model can correctly identify the complete netlist of the circuit, as shown in Fig. 4(a). We use task *topology*.

Accurate identification of elements, connectivity, and ports is fundamental to understanding and analyzing circuits. The complexity of element types and their connections in schematics makes this task particularly challenging. It requires the MLLM to have a more rigorous perception capability compared to traditional visual counting tasks.

The analysis tasks in AMSbench primarily assess the MLLMs’ comprehension of circuit schematics. This includes recognizing and analyzing the functions of circuits, as well as identifying key functional building blocks within them, as illustrated in Fig. 4(b). Additionally, we evaluate the understanding of trade-offs between different circuit performances by both LLMs and MLLMs. Accurately analyzing a circuit and its corresponding performance metrics is the foundation for ensuring accurate and effective circuit design.

The design tasks in our study consider both circuit design and testbench design, as shown in Fig. 5. Proper circuit design ensures that the functionality meets specifications, while effective testbench design guarantees that the circuit’s performance can be accurately measured and validated. These two tasks are central to the AI-driven automation of AMS circuit design. In setting up the circuit design tasks, we adopt and expand upon the benchmark established by AnalogCoder [10].

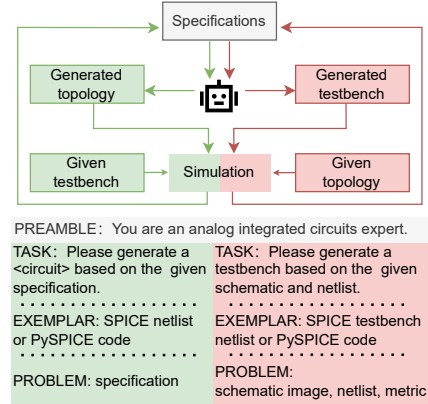


Figure 5: Design task flow

Difficulty Levels We classify the questions into three difficulty levels. Specifically, for the **perception** task, we categorize the difficulty based on the number of elements in the circuit: simple ($\text{num} < 9$), medium ($9 < \text{num} < 16$), and difficult ($\text{num} > 16$). For circuit functionality **analysis**, we classify the problems according to the circuit type and group them into two levels based on their appearance in educational stages: undergraduate and graduate levels. For testing the trade-offs between circuit performances, we assign a classification suitable for engineers. For the **design** task, we classify the circuits based on their complexity into three levels: simple, complex, and system-level circuits.

| Circuit Type | # of Tasks | Circuit Type | # of Tasks | Circuit Type | # of Tasks | Circuit Type | # of Tasks |
|----------------|------------|----------------|------------|-----------------|------------|--------------|------------|
| Amplifier | 7 / 0 / 0 | Oscillator | 0 / 2 / 0 | Subtractor | 0 / 1 / 0 | LDO | 0 / 1 / 0 |
| Inverter | 2 / 0 / 0 | Integrator | 0 / 1 / 0 | Schmitt trigger | 0 / 1 / 0 | Comparator | 0 / 1 / 0 |
| Current mirror | 2 / 0 / 0 | Differentiator | 0 / 1 / 0 | VCO | 0 / 1 / 0 | PLL | 0 / 0 / 1 |
| Op-amp | 2 / 2 / 0 | Adder | 0 / 1 / 0 | Bandgap | 0 / 1 / 0 | SAR-ADC | 0 / 0 / 1 |

Table 1: Circuit design tasks. Number of (simple / complex / system-level) tasks are shown for each circuit type.

| ID | Circuit Type | # of Metrics | ID | Circuit Type | # of Metrics | ID | Circuit Type | # of Metrics |
|----|--------------------------------------|--------------|----|--------------|--------------|----|--------------------|--------------|
| 1 | Cross-coupled differential amplifier | 7 | 5 | PLL | 2 | 9 | Unit capacitor | 1 |
| 2 | Comparator | 2 | 6 | MOS_Ron | 1 | 10 | Folded cascode OTA | 5 |
| 3 | Bootstrap | 1 | 7 | LDO | 7 | 11 | SAR-ADC | 1 |
| 4 | Telescopic cascode OTA | 7 | 8 | VCO | 2 | 12 | Bandgap | 4 |

Table 2: Testbench design tasks with number of metrics required per testbench suite.

3.3 AMSbench Statistics

Fig. 6 illustrates the subtasks involved in the perception task along with the number of questions at varying difficulty levels. Fig. 7 presents statistical information for the analysis task and its various subtasks. The VQA tasks focus on evaluating the MLLM’s ability to interpret circuit schematic images, while the TQA tasks assess the model’s understanding of circuit knowledge and its awareness of performance trade-offs. Table 1 and 25 present an overview of the design tasks for circuits and testbenches, respectively. For the circuit design section, we incorporated the benchmarks provided by AnalogCoder [10] and further extended them with additional circuit tasks, including system-level circuit design. The testbench design tasks address a notable gap in the current community by introducing a previously underexplored category.

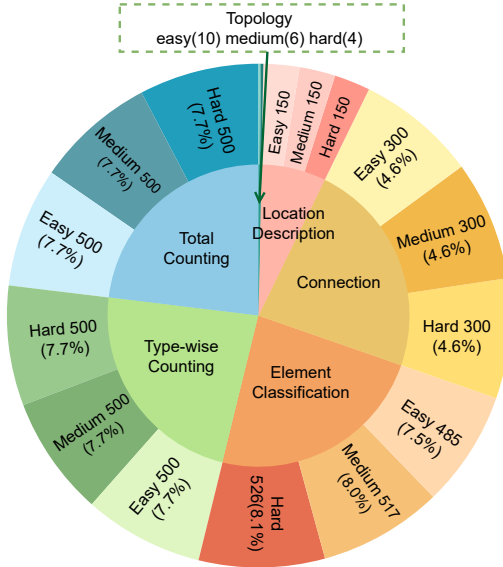


Figure 6: Data statistic of perception task

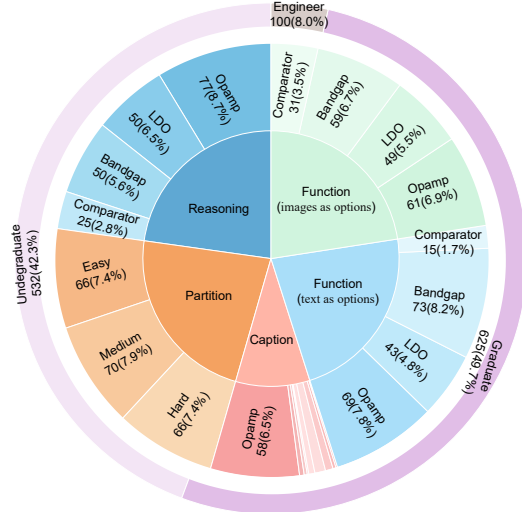


Figure 7: Data statistic of analysis task

4 Experiments

4.1 Models

We perform experiments on mainstream closed-source MLLMs: GPT4o [13], Grok-3 [33], Gemini-2.5-pro [34], Claude3.7 sonnet [35], Doubao-1.5-vision-pro-32k [36], and open-source models: Kimi-VL [37], Qwen2.5-VL 72B [14], DeepSeek-R1 [38]. We evaluate both TQA tasks on all models, and VQA tasks on all models except DeepSeek-R1. We use all open-source models with default parameters and deploy on up to 8 A100 GPUs.

4.2 Metrics

For multiple-choice questions, we adopt accuracy (ACC) as the evaluation metric. For multiple-selection questions, we use the F1 score. For netlist recognition tasks, we define a Netlist Edit Distance (NED) as the evaluation metric, with the calculation procedure illustrated in Fig. 8. The

NED for each schematic image is normalized as shown in (1):

$$\text{NED}_{\text{norm}} = \frac{|\text{GT} \cup \text{Pred}| - |\text{GT} \cap \text{Pred}|}{|\text{GT}|} \quad (1)$$

For evaluating the circuit design and testbench generation tasks, we use $\text{pass}@k$ as the primary metric to measure the success rate of model-generated solutions. The $\text{pass}@k$ metric is calculated as follows. For a given problem, the model generates k distinct answers. The $\text{pass}@k$ value is determined by dividing the number of answers that pass the simulation check by k . For instance, if $k=5$ answers are generated and 3 pass, then $\text{pass}@5 = 3/5 = 0.6$. Additionally, each task is evaluated through 5 repeated experiments, with the average of the $\text{pass}@k$ values taken as the final result.

4.3 Experimental Results

Perception Tasks: Table 3 presents the models’ performance on fundamental circuit schematic recognition tasks. Specifically, component counting and classification, both of which are essential for accurate netlist extraction. Gemini achieves the best overall results. However, due to the complexity and diversity of component types, the models show limitations in accurate counting. For component type classification, Gemini performs well, reaching 94% accuracy. Among open-source models, Qwen2.5-VL achieves 86%, suggesting that open-source models still have room for improvement in component type recognition.

Table 4 presents the accuracy of MLLMs in identifying inter-device connectivity. While the models can produce reasonably accurate predictions for local connections, they fall short in reconstructing the complete netlist. Even netlists produced by the best-performing model, Gemin-2.5-Pro, require substantial modifications to align with the ground truth. Closed-source models perform significantly better on these tasks, whereas some of the open-source models fail to produce outputs in the correct format.

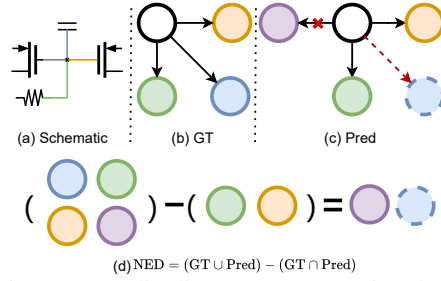


Figure 8: Edit distance computation between the GT netlist and the predicted netlist. The graph illustrates inter-device connections with each device abstracted as a node.

| Models | Total Counting | | Type-wise Counting | | Element Classification | Location Description |
|-----------------------|----------------|--------------|--------------------|--------------|------------------------|----------------------|
| | ACC (↑) | MSE (↓) | ACC (↑) | MSE (↓) | ACC (↑) | ACC (↑) |
| Gemini-2.5-pro | 0.65 | 10.02 | 0.64 | 13.41 | 0.94 | 0.61 |
| GPT-4o | 0.51 | 19.05 | 0.54 | 28.18 | 0.91 | 0.37 |
| Claude-3.7-sonnet | 0.36 | 18.38 | 0.55 | 24.18 | 0.83 | 0.48 |
| Grok-3 | 0.22 | 60.71 | 0.50 | 26.48 | 0.84 | 0.50 |
| Doubao-1.5-vision-pro | 0.24 | 38.13 | 0.51 | 24.76 | 0.93 | 0.45 |
| Kimi-VL-A3B | 0.15 | 49.19 | 0.44 | 34.96 | 0.66 | 0.31 |
| Qwen2.5-VL-72B | 0.43 | 19.59 | 0.49 | 18.59 | 0.86 | 0.56 |

Table 3: Comparison of models across various perception tasks

Analysis Tasks: Table 5 summarizes the models’ capabilities of analyzing AMS circuits, including schematic interpretation and understanding of trade-offs in circuit performance. In schematic interpretation, different MLLMs exhibit distinct strengths: Gemini demonstrates the highest accuracy in identifying and analyzing functional building blocks, while Grok-3 provides more accurate overall descriptions of circuit behavior. Table 16 shows that current models can achieve relatively high accuracy in analyzing circuit knowledge designed for undergraduate and graduate education. However, they perform poorly in understanding the trade-offs between circuit performance metrics commonly encountered in industry. Even the best-performing model, GPT-4o, only achieves 58% accuracy, indicating that LLMs currently lack a clear understanding of the expected performance characteristics of each circuit in the design process.

| Models | Connection Judgment | Connection Identification | Topology |
|-----------------------|---------------------|---------------------------|----------------------|
| | ACC (\uparrow) | F1 (\uparrow) | NED (\downarrow) |
| Gemini-2.5-pro | 0.85 | 0.88 | 0.91 |
| GPT-4o | 0.73 | 0.65 | 1.40 |
| Claude-3.7-sonnet | 0.76 | 0.71 | 1.65 |
| Grok-3 | 0.70 | 0.65 | 1.84 |
| Doubao-1.5-vision-pro | 0.76 | 0.64 | 1.57 |
| Kimi-VL-A3B | 0.53 | 0.53 | – |
| Qwen2.5-VL-72B | 0.77 | 0.52 | 2.38 |

Table 4: Comparison of models on recognizing AMS circuit interconnects

| Models | Reasoning Partition | | Caption | Function (text) | Function (image) | TQA |
|-----------------------|---------------------|-------------------|--------------------|--------------------|--------------------|--------------------|
| | ACC (\uparrow) | F1 (\uparrow) | ACC (\uparrow) | ACC (\uparrow) | ACC (\uparrow) | ACC (\uparrow) |
| Gemini-2.5-pro | 0.92 | 0.80 | 0.70 | 0.95 | 0.94 | 0.72 |
| GPT-4o | 0.77 | 0.57 | 0.61 | 0.93 | 0.89 | 0.78 |
| Claude-3.7-sonnet | 0.91 | 0.64 | 0.98 | 0.88 | 0.74 | 0.74 |
| Grok-3 | 0.61 | 0.59 | 0.41 | 0.77 | 0.22 | 0.74 |
| Doubao-1.5-vision-pro | 0.83 | 0.60 | 0.70 | 0.94 | 0.93 | 0.76 |
| Kimi-VL-A3B | 0.74 | 0.25 | 0.71 | 0.59 | 0.28 | 0.59 |
| Qwen2.5-VL-72B | 0.82 | 0.45 | 0.78 | 0.78 | 0.85 | 0.69 |

Table 5: Comparison of models on Reasoning, Partition Identification, Caption Generation, Function, and TQA tasks

Design Tasks: Table 6 shows the performance of the models in circuit design and testbench design tasks. For circuit design, Grok-3 and Claude-Sonnet achieve the best results. However, for testbench design, none of the current models can directly generate syntactically correct testbenches, with only occasionally exceptions of GPT-4o. One possible reason is that the current pretraining data lacks sufficient testbench-related knowledge. Additionally, the metrics that need to be measured vary across different circuits, making testbench generation highly challenging.

5 Observation and Findings

Based on the models’ performance across various tasks, we summarize and analyze the current challenges faced by Multimodal Large Language Models (MLLMs) in the field of AMS circuit from the dimensions of perception, analysis, and design.

Perception Tasks: Existing MLLMs remain incapable of accurately interpreting circuit schematics. While certain models demonstrate promising performance in capturing localized connectivity patterns, their effectiveness significantly deteriorates when tasked with comprehensive netlist extraction. Fig. 23 in the appendix gives such an example. A primary challenge is that MLLMs are inaccurate in assigning connection points (i.e. pins and ports) to their parent components, resulting in various connectivity errors.

Analysis Tasks: Some MLLMs demonstrate reasonable levels of circuit analysis capability. They accurately interpret circuit functionalities, which indicates a comprehensive and precise understanding of circuit knowledge, as well as a degree of generalization in visual recognition when dealing with

| Model | Circuit Design | | | Testbench Design | |
|-----------------------|----------------|-------------|-------------|------------------|----------|
| | Pass@3 | Pass@5 | Pass@10 | Syntax@5 | Metric@5 |
| Gemini-2.5-pro | 0.57 | 0.54 | 0.43 | 0 | 0 |
| GPT-4o | 0.47 | 0.49 | 0.42 | 0.084 | 0 |
| Claude-3.7-sonnet | 0.63 | 0.64 | 0.50 | 0 | 0 |
| Grok-3 | 0.65 | 0.54 | 0.61 | 0 | 0 |
| Doubao-1.5-vision-pro | 0.45 | 0.24 | 0.15 | 0 | 0 |
| Qwen2.5-VL-72B | 0.47 | 0.41 | 0.33 | 0 | 0 |
| Kimi-VL-A3B | 0.41 | 0.25 | 0.13 | 0 | 0 |
| DeepSeek-R1 | 0.55 | 0.51 | 0.45 | - | - |

Table 6: Comparison of models and circuit design and testbench design tasks. The data presents the average results of all the circuits listed in Table 1. Detailed results are available in the appendix in Tables 18-27. *Syntax*: generated testbench is syntactically correct to run simulation. *Metric*: generated testbench is topologically and parametrically correct and produces the correct performance metric.

stylized images. Nevertheless, for the reasoning tasks, the models occasionally produce correct answers despite evident errors in their analytical process, which undermines our confidence in their correct answers. For instance, when examining an operational amplifier circuit diagram comprising over 15 components, models may inaccurately identify the IDs of transistor elements responsible for forming the current mirror, erroneously recognizing M1–M2 as M3–M4. This misidentification aligns with the model’s observed performance in tasks involving component counting and device classification. Possible reasons include: 1. The model exhibits hallucinations when recognizing circuit diagrams with a large number of components [39]. 2. Models generally prioritize global information capture, often at the expense of local information, which is crucial for nuanced understanding [40].

In the circuit design process, particularly during the sizing and layout auto-generation stages, a model with strong circuit analysis abilities can significantly reduce the parameter search space and enable partitioning of the circuit into macros for efficient layout generation. However, the current model lacks the ability to accurately quantify the trade-offs between circuit performance metrics, which limits its capability to recommend the appropriate circuit topology when given a target specification.

Design Tasks: Our evaluation findings show that current models perform well in simple circuit design tasks but struggle with complex and system-level circuits, such as the Successive Approximation Register Analog-to-Digital Converter (SAR-ADC). For system-level circuits, most model-generated designs fail the netlist rule check, which verifies the accuracy of component interconnections. Additionally, none of the designs meet the specified circuit performance criteria. A comprehensive analysis of the SAR-ADC design produced by the GPT-4o model, which demonstrates comparatively robust performance across diverse tasks, is presented in Fig. 29 in the appendix. The circuit schematic indicates that GPT-4o accurately implements the differential input structure. However, due to an incomplete understanding of the SAR-ADC’s operating principles, the model was unable to extend the design beyond the differential input pair, resulting in an extremely incomplete circuit.

6 Conclusion and Future Work

This paper introduces AMSbench, a benchmark designed to evaluate the capabilities of MLLMs in the AMS circuit domain. The benchmark comprehensively assesses model performance across three key dimensions—schematic perception, circuit analysis, and circuit design—covering a variety of tasks. AMSbench reveals significant limitations in current MLLMs, especially in schematic perception and complex circuit design. While certain models perform adequately in basic component recognition and simpler circuit analysis tasks, they notably struggle with advanced tasks, including accurate schematic interpretation and system-level circuit design.

Given the increasing interest in applying MLLMs to automate AMS design processes, AMSbench provides an essential evaluation framework, establishing a robust foundation for future advancements

in this field. Achieving high-performance scores on AMSbench would signify substantial progress and tangible benefits in the automation of AMS circuit design.

Looking ahead, we plan to expand AMSbench by including additional AMS circuits and covering more stages of the circuit design lifecycle, such as sizing and layout design. Furthermore, we aim to introduce evaluation tasks involving analysis of simulation result statistics and visual plots, aligning more closely with the inherently interactive nature of practical circuit design. This expansion will facilitate a deeper understanding of end-to-end circuit design processes and enable more comprehensive assessments of emerging methodologies.

References

- [1] C. Cui, Y. Ma, X. Cao, W. Ye, Y. Zhou, K. Liang, J. Chen, J. Lu, Z. Yang, K.-D. Liao, *et al.*, “A Survey on Multimodal Large Language Models for Autonomous Driving,” in *Proceedings of the IEEE/CVF Winter Conference on Applications of Computer Vision*, pp. 958–979, 2024.
- [2] Y. Hao, J. Gu, H. W. Wang, L. Li, Z. Yang, L. Wang, and Y. Cheng, “Can MLLMs Reason in Multimodality? EMMA: An Enhanced MultiModal Reasoning Benchmark,” *arXiv preprint arXiv:2501.05444*, 2025.
- [3] X. Yue, Y. Ni, T. Zheng, K. Zhang, R. Liu, G. Zhang, S. Stevens, D. Jiang, W. Ren, Y. Sun, *et al.*, “MMMU: A Massive Multi-Discipline Multimodal Understanding and Reasoning Benchmark for Expert AGI,” in *Proceedings of the IEEE/CVF Conference on Computer Vision and Pattern Recognition*, pp. 9556–9567, 2024.
- [4] R. Zhang, D. Jiang, Y. Zhang, H. Lin, Z. Guo, P. Qiu, A. Zhou, P. Lu, K.-W. Chang, Y. Qiao, *et al.*, “MathVerse: Does Your Multi-modal LLM Truly See the Diagrams in Visual Math Problems?,” in *European Conference on Computer Vision*, pp. 169–186, Springer, 2024.
- [5] P. Lu, H. Bansal, T. Xia, J. Liu, C. Li, H. Hajishirzi, H. Cheng, K.-W. Chang, M. Galley, and J. Gao, “MathVista: Evaluating Math Reasoning in Visual Contexts with GPT-4V, Bard, and Other Large Multimodal Models,” *CoRR*, 2023.
- [6] A. Yang, B. Zhang, B. Hui, B. Gao, B. Yu, C. Li, D. Liu, J. Tu, J. Zhou, J. Lin, *et al.*, “Qwen2.5-Math Technical Report: Toward Mathematical Expert Model via Self-Improvement,” *arXiv preprint arXiv:2409.12122*, 2024.
- [7] L. Zhong and Z. Wang, “Can LLM Replace Stack Overflow? A Study on Robustness and Reliability of Large Language Model Code Generation,” in *Proceedings of the AAAI Conference on Artificial Intelligence*, vol. 38, pp. 21841–21849, 2024.
- [8] J. Bhandari, V. Bhat, Y. He, H. Rahmani, S. Garg, and R. Karri, “Masala-chai: A large-scale spice netlist dataset for analog circuits by harnessing ai,” 2025.
- [9] J. Gao, W. Cao, J. Yang, and X. Zhang, “AnalogGenie: A Generative Engine for Automatic Discovery of Analog Circuit Topologies,” *arXiv preprint arXiv:2503.00205*, 2025.
- [10] Y. Lai, S. Lee, G. Chen, S. Poddar, M. Hu, D. Z. Pan, and P. Luo, “Analogcoder: Analog circuit design via training-free code generation,” in *Proceedings of the AAAI Conference on Artificial Intelligence*, vol. 39, pp. 379–387, 2025.
- [11] Z. Chen, J. Huang, Y. Liu, F. Yang, L. Shang, D. Zhou, and X. Zeng, “Artisan: Automated Operational Amplifier Design via Domain-specific Large Language Model,” in *2024 61th ACM/IEEE Design Automation Conference (DAC)*, pp. 1–6, 2024.
- [12] Z. Tao, Y. Shi, Y. Huo, R. Ye, Z. Li, L. Huang, C. Wu, N. Bai, Z. Yu, T.-J. Lin, *et al.*, “Amsnet: Netlist dataset for ams circuits,” in *2024 IEEE LLM Aided Design Workshop (LAD)*, pp. 1–5, IEEE, 2024.
- [13] A. Hurst, A. Lerer, A. P. Goucher, A. Perelman, A. Ramesh, A. Clark, A. Ostrow, A. Welihinda, A. Hayes, A. Radford, *et al.*, “Gpt-4o system card,” *arXiv preprint arXiv:2410.21276*, 2024.
- [14] A. Yang, B. Yang, B. Zhang, B. Hui, B. Zheng, B. Yu, C. Li, D. Liu, F. Huang, H. Wei, *et al.*, “Qwen2.5 technical report,” *arXiv preprint arXiv:2412.15115*, 2024.

- [15] C. Liu, W. Chen, A. Peng, Y. Du, L. Du, and J. Yang, “AmpAgent: An LLM-based Multi-Agent System for Multi-stage Amplifier Schematic Design from Literature for Process and Performance Porting,” *arXiv preprint arXiv:2409.14739*, 2024.
- [16] J. Chaudhuri, D. Thapar, A. Chaudhuri, F. Firouzi, and K. Chakrabarty, “SPICED+: Syntactical Bug Pattern Identification and Correction of Trojans in A/MS Circuits Using LLM-Enhanced Detection,” *IEEE Transactions on Very Large Scale Integration (VLSI) Systems*, 2025.
- [17] Z. Yan, Y. Qin, X. S. Hu, and Y. Shi, “On the viability of using llms for sw/hw co-design: An example in designing cim dnn accelerators,” in *2023 IEEE 36th International System-on-Chip Conference (SOCC)*, pp. 1–6, IEEE, 2023.
- [18] J. Blocklove, S. Garg, R. Karri, and H. Pearce, “Chip-chat: Challenges and opportunities in conversational hardware design,” in *2023 ACM/IEEE 5th Workshop on Machine Learning for CAD (MLCAD)*, pp. 1–6, IEEE, 2023.
- [19] Y. Fu, Y. Zhang, Z. Yu, S. Li, Z. Ye, C. Li, C. Wan, and Y. C. Lin, “Gpt4aigchip: Towards next-generation ai accelerator design automation via large language models,” in *2023 IEEE/ACM International Conference on Computer Aided Design (ICCAD)*, pp. 1–9, IEEE, 2023.
- [20] J. Pan, G. Zhou, C.-C. Chang, I. Jacobson, J. Hu, and Y. Chen, “A Survey of Research in Large Language Models for Electronic Design Automation,” *ACM Transactions on Design Automation of Electronic Systems*, 2025.
- [21] W. Fang, J. Wang, Y. Lu, S. Liu, Y. Wu, Y. Ma, and Z. Xie, “A survey of circuit foundation model: Foundation ai models for vlsi circuit design and eda,” *arXiv preprint arXiv:2504.03711*, 2025.
- [22] L. Ouyang, J. Wu, X. Jiang, D. Almeida, C. Wainwright, P. Mishkin, C. Zhang, S. Agarwal, K. Slama, A. Ray, *et al.*, “Training language models to follow instructions with human feedback,” *Advances in neural information processing systems*, vol. 35, pp. 27730–27744, 2022.
- [23] Y. Yin, Y. Wang, B. Xu, and P. Li, “ADO-LLM: Analog Design Bayesian Optimization with In-Context Learning of Large Language Models,” *arXiv preprint arXiv:2406.18770*, 2024.
- [24] Y. Shi, Z. Tao, Y. Gao, T. Zhou, C. Chang, Y. Wang, B. Chen, G. Zhang, A. Liu, Z. Yu, *et al.*, “AMSnet-KG: A Netlist Dataset for LLM-based AMS Circuit Auto-Design Using Knowledge Graph RAG,” *arXiv preprint arXiv:2411.13560*, 2024.
- [25] M. Liu, N. Pinckney, B. Khailany, and H. Ren, “VerilogEval: Evaluating Large Language Models for Verilog Code Generation,” in *2023 IEEE/ACM International Conference on Computer-Aided Design (ICCAD)*, 2023.
- [26] Y. Lu, S. Liu, Q. Zhang, and Z. Xie, “RTLML: An Open-Source Benchmark for Design RTL Generation with Large Language Model,” in *2024 29th Asia and South Pacific Design Automation Conference (ASP-DAC)*, pp. 722–727, IEEE, 2024.
- [27] L. Skelic, Y. Xu, M. Cox, W. Lu, T. Yu, and R. Han, “CIRCUIT: A Benchmark for Circuit Interpretation and Reasoning Capabilities of LLMs,” *arXiv preprint arXiv:2502.07980*, 2025.
- [28] B. Razavi, *Design of Analog CMOS Integrated Circuits*. McGraw-Hill Higher Education, 2005.
- [29] P. R. Gray, P. J. Hurst, S. H. Lewis, and R. G. Meyer, *Analysis and Design of Analog Integrated Circuits*. John Wiley & Sons, 2009.
- [30] P. E. Allen and D. R. Holberg, *CMOS Analog Circuit Design*. Elsevier, 2011.
- [31] W. M. Sansen, *Analog Design Essentials*, vol. 859. Springer Science & Business Media, 2007.
- [32] B. Wang, C. Xu, X. Zhao, L. Ouyang, F. Wu, Z. Zhao, R. Xu, K. Liu, Y. Qu, F. Shang, *et al.*, “Mineru: An open-source solution for precise document content extraction,” 2024.
- [33] “Grok 3 beta—the age of reasoning agents.” <https://x.ai/blog/grok-3>, 2025. Accessed: 2025-05-14.

- [34] G. Team, R. Anil, S. Borgeaud, J.-B. Alayrac, J. Yu, R. Soricut, J. Schalkwyk, A. M. Dai, A. Hauth, K. Millican, *et al.*, “Gemini: a family of highly capable multimodal models,” *arXiv preprint arXiv:2312.11805*, 2023.
- [35] Anthropic, “Introducing claude 3.7 sonnet.” <https://www.anthropic.com/news/>, 2024. Accessed: 2025-05-14.
- [36] D. Guo, F. Wu, F. Zhu, F. Leng, G. Shi, H. Chen, H. Fan, J. Wang, J. Jiang, J. Wang, *et al.*, “Seed1. 5-VL Technical Report,” *arXiv preprint arXiv:2505.07062*, 2025.
- [37] K. Team, A. Du, B. Yin, B. Xing, B. Qu, B. Wang, C. Chen, C. Zhang, C. Du, C. Wei, *et al.*, “Kimi-VL Technical Report,” *arXiv preprint arXiv:2504.07491*, 2025.
- [38] D. Guo, D. Yang, H. Zhang, J. Song, R. Zhang, R. Xu, Q. Zhu, S. Ma, P. Wang, X. Bi, *et al.*, “Deepseek-r1: Incentivizing reasoning capability in llms via reinforcement learning,” *arXiv preprint arXiv:2501.12948*, 2025.
- [39] Y. Zhou, C. Cui, J. Yoon, L. Zhang, Z. Deng, C. Finn, M. Bansal, and H. Yao, “Analyzing and Mitigating Object Hallucination in Large Vision-Language Models,” *arXiv preprint arXiv:2310.00754*, 2023.
- [40] Z. Li, Q. Xu, D. Zhang, H. Song, Y. Cai, Q. Qi, R. Zhou, J. Pan, Z. Li, V. Tu, *et al.*, “Groundinggpt: Language enhanced multi-modal grounding model,” in *Proceedings of the 62nd Annual Meeting of the Association for Computational Linguistics (Volume 1: Long Papers)*, pp. 6657–6678, 2024.

A Detailed Experiment Results

A.1 Results of perception tasks

| Models | Metric | Counting Task | | | | | | | |
|-----------------------|----------------------|----------------|-------------|--------------|--------------|--------------------|-------------|--------------|--------------|
| | | Total Counting | | | | Type-wise Counting | | | |
| | | Easy | Medium | Hard | Total | Easy | Medium | Hard | Total |
| Gemini-2.5-pro | ACC (\uparrow) | 0.88 | 0.65 | 0.45 | 0.65 | 0.83 | 0.63 | 0.46 | 0.64 |
| | MSE (\downarrow) | 0.39 | 2.30 | 27.36 | 10.02 | 0.67 | 3.75 | 35.81 | 13.41 |
| GPT-4o | ACC (\uparrow) | 0.75 | 0.51 | 0.26 | 0.51 | 0.76 | 0.57 | 0.30 | 0.54 |
| | MSE (\downarrow) | 0.80 | 2.63 | 53.72 | 19.05 | 2.15 | 6.96 | 75.44 | 28.18 |
| Claude-3.7-sonnet | ACC (\uparrow) | 0.72 | 0.27 | 0.01 | 0.36 | 0.73 | 0.57 | 0.35 | 0.55 |
| | MSE (\downarrow) | 0.56 | 3.63 | 50.96 | 18.38 | 2.29 | 6.67 | 63.57 | 24.18 |
| Grok-3 | ACC (\uparrow) | 0.47 | 0.14 | 0.04 | 0.22 | 0.70 | 0.53 | 0.27 | 0.50 |
| | MSE (\downarrow) | 3.58 | 21.50 | 157.05 | 60.71 | 2.49 | 6.92 | 68.51 | 26.48 |
| Doubao-1.5-vision-pro | ACC (\uparrow) | 0.60 | 0.10 | 0.01 | 0.24 | 0.71 | 0.53 | 0.30 | 0.51 |
| | MSE (\downarrow) | 0.67 | 5.93 | 107.78 | 38.13 | 2.56 | 9.14 | 62.59 | 24.76 |
| Kimi-VL-A3B | ACC (\uparrow) | 0.23 | 0.13 | 0.08 | 0.15 | 0.63 | 0.46 | 0.23 | 0.44 |
| | MSE (\downarrow) | 15.68 | 28.04 | 103.86 | 49.19 | 2.86 | 13.44 | 94.38 | 34.96 |
| Qwen2.5-VL-72B | ACC (\uparrow) | 0.67 | 0.42 | 0.21 | 0.43 | 0.68 | 0.47 | 0.31 | 0.49 |
| | MSE (\downarrow) | 1.09 | 3.98 | 53.90 | 19.59 | 1.87 | 6.55 | 47.35 | 18.59 |

Table 7: Counting Task Performance Across Different Models

| Models | Element Classification Task (ACC \uparrow) | | | |
|-----------------------|---|-------------|-------------|-------------|
| | Easy | Medium | Hard | Total |
| Gemini-2.5-pro | 0.96 | 0.94 | 0.91 | 0.94 |
| GPT-4o | 0.93 | 0.93 | 0.88 | 0.91 |
| Claude-3.7-sonnet | 0.90 | 0.87 | 0.84 | 0.83 |
| Grok-3 | 0.84 | 0.84 | 0.83 | 0.84 |
| Doubao-1.5-vision-pro | 0.94 | 0.93 | 0.91 | 0.93 |
| Kimi-VL-A3B | 0.69 | 0.65 | 0.63 | 0.66 |
| Qwen2.5-VL-72B | 0.88 | 0.86 | 0.83 | 0.86 |

Table 8: Element Classification Task Performance Across Different Models (in decimals)

| Models | Metric | Interconnect Perception Task | | | | | | | |
|-----------------------|--------------------|------------------------------|-------------|-------------|-------------|---------------------------|-------------|-------------|-------------|
| | | Connection Judgment | | | | Connection Identification | | | |
| | | Easy | Medium | Hard | Total | Easy | Medium | Hard | Total |
| Gemini-2.5-pro | ACC (\uparrow) | 0.86 | 0.83 | 0.85 | 0.85 | 0.78 | 0.51 | 0.50 | 0.60 |
| | F1 (\uparrow) | - | - | - | - | 0.93 | 0.86 | 0.86 | 0.88 |
| GPT-4o | ACC (\uparrow) | 0.74 | 0.71 | 0.74 | 0.73 | 0.27 | 0.12 | 0.10 | 0.16 |
| | F1 (\uparrow) | - | - | - | - | 0.74 | 0.61 | 0.59 | 0.65 |
| Claude-3.7-sonnet | ACC (\uparrow) | 0.74 | 0.76 | 0.77 | 0.76 | 0.36 | 0.25 | 0.22 | 0.27 |
| | F1 (\uparrow) | - | - | - | - | 0.74 | 0.71 | 0.68 | 0.71 |
| Grok-3 | ACC (\uparrow) | 0.72 | 0.72 | 0.67 | 0.70 | 0.25 | 0.16 | 0.13 | 0.18 |
| | F1 (\uparrow) | - | - | - | - | 0.70 | 0.63 | 0.62 | 0.65 |
| Doubao-1.5-vision-pro | ACC (\uparrow) | 0.78 | 0.74 | 0.77 | 0.76 | 0.30 | 0.13 | 0.14 | 0.19 |
| | F1 (\uparrow) | - | - | - | - | 0.72 | 0.60 | 0.59 | 0.64 |
| Kimi-VL-A3B | ACC (\uparrow) | 0.55 | 0.54 | 0.51 | 0.53 | 0.13 | 0.09 | 0.10 | 0.10 |
| | F1 (\uparrow) | - | - | - | - | 0.57 | 0.51 | 0.52 | 0.53 |
| Qwen2.5-VL-72B | ACC (\uparrow) | 0.75 | 0.78 | 0.77 | 0.77 | 0.20 | 0.10 | 0.13 | 0.14 |
| | F1 (\uparrow) | - | - | - | - | 0.56 | 0.48 | 0.53 | 0.52 |

Table 9: Interconnect Perception Task Performance Across Different Models

| Models | Location Description Task (ACC \uparrow) | | | |
|-----------------------|---|-------------|-------------|-------------|
| | Easy | Medium | Hard | Total |
| Gemini-2.5-pro | 0.61 | 0.60 | 0.61 | 0.61 |
| GPT-4o | 0.44 | 0.31 | 0.37 | 0.37 |
| Claude-3.7-sonnet | 0.49 | 0.45 | 0.50 | 0.48 |
| Grok-3 | 0.45 | 0.55 | 0.49 | 0.50 |
| Doubao-1.5-vision-pro | 0.51 | 0.47 | 0.38 | 0.45 |
| Kimi-VL-A3B | 0.32 | 0.33 | 0.27 | 0.31 |
| Qwen2.5-VL-72B | 0.57 | 0.59 | 0.53 | 0.56 |

Table 10: Location Description Task Performance Across Different Models

| Models | Topology Generation Task (NED \downarrow) | | | |
|-----------------------|--|-------------|-------------|-------------|
| | Easy | Medium | Hard | Total |
| Gemini-2.5-pro | 0.73 | 0.95 | 1.34 | 0.91 |
| GPT-4o | 1.31 | 1.56 | 1.46 | 1.40 |
| Claude-3.7-sonnet | 1.72 | 1.64 | 1.51 | 1.65 |
| Grok-3 | 2.08 | 1.71 | 1.37 | 1.84 |
| Doubao-1.5-vision-pro | 1.54 | 1.52 | 1.68 | 1.57 |
| Kimi-VL-A3B | – | – | – | – |
| Qwen2.5-VL-72B | 2.65 | 2.14 | 1.95 | 2.38 |

Table 11: Topology Generation Task Performance Across Different Models

A.2 Results of analysis tasks

| Models | Function Identification Task (ACC \uparrow) | |
|-----------------------|--|-----------------------------|
| | Function (text as options) | Function (image as options) |
| Gemini-2.5-pro | 0.95 | 0.94 |
| GPT-4o | 0.93 | 0.89 |
| Claude-3.7-sonnet | 0.88 | 0.74 |
| Grok-3 | 0.77 | 0.22 |
| Doubao-1.5-vision-pro | 0.94 | 0.93 |
| Kimi-VL-A3B | 0.59 | 0.28 |
| Qwen2.5-VL-72B | 0.78 | 0.85 |

Table 12: Function Identification Task Performance Across Different Models

| Models | Circuit Partition Task | | | | | | | |
|-----------------------|------------------------|---------------|----------------|---------------|----------------|---------------|----------------|---------------|
| | Easy | | Medium | | Hard | | Overall | |
| | ACC \uparrow | F1 \uparrow | ACC \uparrow | F1 \uparrow | ACC \uparrow | F1 \uparrow | ACC \uparrow | F1 \uparrow |
| Gemini-2.5-pro | 0.52 | 0.81 | 0.33 | 0.81 | 0.20 | 0.78 | 0.35 | 0.80 |
| GPT-4o | 0.21 | 0.55 | 0.07 | 0.59 | 0.06 | 0.57 | 0.11 | 0.57 |
| Claude-3.7-sonnet | 0.29 | 0.66 | 0.11 | 0.62 | 0.08 | 0.62 | 0.16 | 0.64 |
| Grok-3 | 0.26 | 0.59 | 0.17 | 0.63 | 0.03 | 0.56 | 0.15 | 0.59 |
| Doubao-1.5-vision-pro | 0.26 | 0.63 | 0.04 | 0.61 | 0.03 | 0.54 | 0.11 | 0.60 |
| Kimi-VL-A3B | 0.03 | 0.29 | 0.00 | 0.00 | 0.00 | 0.00 | 0.00 | 0.28 |
| Qwen2.5-VL-72B | 0.06 | 0.44 | 0.00 | 0.49 | 0.00 | 0.43 | 0.02 | 0.45 |

Table 13: Circuit Partition Task Performance Across Different Models

| Models | Reasoning Task (ACC \uparrow) | | | |
|-----------------------|----------------------------------|-------------|-------------|-------------|
| | Op-amp | LDO | Bandgap | Comparator |
| Gemini-2.5-pro | 0.94 | 0.90 | 0.88 | 0.96 |
| GPT-4o | 0.78 | 0.84 | 0.64 | 0.84 |
| Claude-3.7-sonnet | 0.95 | 0.96 | 0.78 | 0.96 |
| Grok-3 | 0.60 | 0.72 | 0.52 | 0.60 |
| Doubao-1.5-vision-pro | 0.90 | 0.84 | 0.80 | 0.80 |
| Kimi-VL-A3B | 0.81 | 0.46 | 0.86 | 0.84 |
| Qwen2.5-VL-72B | 0.81 | 0.90 | 0.72 | 0.84 |

Table 14: Reasoning Task Performance Across Different Models

| Models | Caption Generation Task(ACC \uparrow) | | |
|-----------------------|--|-------------|-------------|
| | Undergraduate | Graduate | Total |
| Gemini-2.5-pro | 0.63 | 0.72 | 0.70 |
| GPT-4o | 0.58 | 0.63 | 0.61 |
| Claude-3.7-sonnet | 0.89 | 1.00 | 0.98 |
| Grok-3 | 0.21 | 0.47 | 0.41 |
| Doubao-1.5-vision-pro | 0.74 | 0.69 | 0.70 |
| Kimi-VL-A3B | 0.74 | 0.70 | 0.71 |
| Qwen2.5-VL-72B | 0.89 | 0.75 | 0.78 |

Table 15: Caption Generation Task Performance Across Different Models

| Models | TQA Task(ACC \uparrow) | | | |
|-----------------------|---------------------------|-------------|-------------|-------------|
| | Undergraduate | Graduate | Engineer | Total |
| Gemini-2.5-pro | 0.89 | 0.89 | 0.39 | 0.72 |
| GPT-4o | 0.88 | 0.88 | 0.58 | 0.78 |
| Claude-3.7-sonnet | 0.90 | 0.88 | 0.45 | 0.74 |
| Grok-3 | 0.86 | 0.84 | 0.53 | 0.74 |
| Doubao-1.5-vision-pro | 0.88 | 0.88 | 0.52 | 0.76 |
| Kimi-VL-A3B | 0.80 | 0.82 | 0.16 | 0.59 |
| Qwen2.5-VL-72B | 0.85 | 0.85 | 0.37 | 0.69 |
| DeepSeek-R1 | 0.89 | 0.90 | 0.58 | 0.77 |

Table 16: TQA Task Performance Across Different Models (Decimal Format)

A.3 Results of design tasks

A.3.1 Circuit Design Task

| Id | Type | Circuit Description | Id | Type | Circuit Description |
|----|----------------|--|----|-----------------|---------------------------------------|
| 1 | Amplifier | Single-stage common-source amp. with R load | 15 | Op-amp | Telescopic cascode op-amp |
| 2 | Amplifier | 3-stage common-source amp. with R load | 16 | Oscillator | RC phase-shift oscillator |
| 3 | Amplifier | Common-drain amp. with R load | 17 | Oscillator | A Wien bridge oscillator |
| 4 | Amplifier | Single-stage common-gate amp. with R load | 18 | Integrator | Op-amp integrator |
| 5 | Amplifier | Single-stage cascode amp. with R load | 19 | Differentiator | Op-amp differentiator |
| 6 | Inverter | NMOS inverter with R load | 20 | Adder | Op-amp adder |
| 7 | Inverter | Logical inverter with NMOS and PMOS | 21 | Subtractor | Op-amp subtractor |
| 8 | Current mirror | NMOS constant current source with R load | 22 | Schmitt trigger | Non-inverting Schmitt trigger |
| 9 | Amplifier | 2-stage amp. with Miller compensation | 23 | VCO | Voltage-controlled oscillator |
| 10 | Amplifier | Common-source amp. with diode-connected load | 24 | Bandgap | A classic brokaw bandgap reference |
| 11 | Op-amp | Differential op-amp with current mirror load | 25 | Comparator | A low offset voltage dual comparator |
| 12 | Current mirror | Cascode current mirror | 26 | LDO | 1A low dropout voltage regulator |
| 13 | Op-amp | Single-stage common-source op-amp with R loads | 27 | PLL | Phase-locked loop |
| 14 | Op-amp | 2-stage differential op-amp with active loads | 28 | SAR-ADC | Successive approximation register ADC |

Table 17: Circuit block library (two parallel lists), with column-specific background coloring(blue means simple, green means complex, red means system level

| Models | 1. Amplifier | | | 2. Amplifier | | | 3. Amplifier | | | 4. Amplifier | | |
|-----------------------|--------------|------|------|--------------|------|------|--------------|------|------|--------------|------|------|
| | p@3 | p@5 | p@10 | p@3 | p@5 | p@10 | p@3 | p@5 | p@10 | p@3 | p@5 | p@10 |
| Gemini-2.5-pro | 1 | 1 | 1 | 1 | 1 | 1 | 0.67 | 0.67 | 0.67 | 1 | 1 | 1 |
| Gpt-4o | 1 | 1 | 1 | 1 | 1 | 1 | 0 | 1 | 1 | 0.33 | 0.33 | 0.33 |
| Claude-3.7-sonnet | 1 | 1 | 1 | 1 | 1 | 1 | 0.33 | 0.67 | 1 | 0.67 | 0.67 | 0.67 |
| Grok-3 | 1 | 1 | 1 | 1 | 1 | 1 | 0 | 1 | 1 | 0.67 | 0.67 | 0.67 |
| Doubao-1.5-vision-pro | 0.67 | 0.67 | 0.67 | 0.43 | 0.43 | 0.43 | 0.33 | 0.33 | 0.33 | 0.13 | 0.13 | 0.13 |
| Kimi-VL-A3B | 0 | 0 | 0 | 0 | 0 | 0 | 0 | 0 | 0 | 0 | 0 | 0 |
| Qwen2.5-VL-72B | 0 | 0 | 0 | 0 | 0 | 0 | 0 | 0 | 0 | 0 | 0 | 0 |

Table 18: Per-circuit pass@k scores (k = 3, 5, 10) for CKT1–CKT4 across multiple models

| Models | 5. Amplifier | | | 6. Inverter | | | 7. Inverter | | | 8. Current mirror | | |
|-----------------------|--------------|------|------|-------------|------|------|-------------|------|------|-------------------|-----|------|
| | p@3 | p@5 | p@10 | p@3 | p@5 | p@10 | p@3 | p@5 | p@10 | p@3 | p@5 | p@10 |
| Gemini-2.5-pro | 1 | 1 | 1 | 1 | 1 | 1 | 1 | 1 | 1 | 1 | 1 | 1 |
| GPT-4o | 1 | 1 | 1 | 1 | 1 | 1 | 1 | 1 | 1 | 1 | 1 | 1 |
| Claude-3.7-sonnet | 1 | 1 | 1 | 1 | 1 | 1 | 1 | 1 | 1 | 1 | 1 | 1 |
| Grok-3 | 1 | 1 | 1 | 1 | 1 | 1 | 1 | 1 | 1 | 1 | 1 | 1 |
| Doubao-1.5-vision-pro | 0.23 | 0.23 | 0.23 | 0.23 | 0.23 | 0.23 | 0.49 | 0.49 | 0.49 | 1 | 1 | 1 |
| Kimi-VL-A3B | 0 | 0 | 0 | 0 | 0 | 0 | 0 | 0 | 0 | 0 | 0 | 0 |
| Qwen2.5-VL-72B | 0 | 0 | 0 | 0 | 0 | 0 | 0 | 0 | 0 | 0 | 0 | 0 |

Table 19: Per-circuit pass@k scores (k = 3, 5, 10) for CKT5–CKT8 across multiple models

| Model | 9. Amplifier | | | 10. Amplifier | | | 11. Op-amp | | | 12. Current mirror | | |
|-----------------------|--------------|------|------|---------------|------|------|------------|------|------|--------------------|------|------|
| | p@3 | p@5 | p@10 | p@3 | p@5 | p@10 | p@3 | p@5 | p@10 | p@3 | p@5 | p@10 |
| Gemini-2.5-pro | 1 | 1 | 1 | 0.61 | 0.61 | 0.61 | 0.48 | 0.48 | 0.48 | 0.24 | 0.24 | 0.24 |
| GPT-4o | 1 | 1 | 1 | 0.43 | 0.43 | 0.43 | 0.22 | 0.22 | 0.22 | 0 | 0 | 0 |
| Claude-3.7-sonnet | 1 | 1 | 1 | 0.87 | 0.87 | 0.87 | 0.65 | 0.65 | 0.65 | 0.62 | 0.62 | 0.62 |
| Grok-3 | 1 | 1 | 1 | 0.86 | 0.86 | 0.86 | 0.29 | 0.29 | 0.29 | 0.33 | 0.33 | 0.33 |
| Doubao-1.5-vision-pro | 0.27 | 0.27 | 0.27 | 0.61 | 0.61 | 0.61 | 0.33 | 0.33 | 0.33 | 0.31 | 0.31 | 0.31 |
| Kimi-VL-A3B | 0 | 0 | 0 | 0 | 0 | 0 | 0 | 0 | 0 | 0 | 0 | 0 |
| Qwen2.5-VL-72B | 0 | 0 | 0 | 0 | 0 | 0 | 0 | 0 | 0 | 0 | 0 | 0 |

Table 20: Per-circuit pass@k scores (k = 3, 5, 10) for CKT9–CKT12 across multiple models

| Model | 13. Op-amp | | | 14. Op-amp | | | 15. Op-amp | | | 16. Oscillator | | |
|-----------------------|------------|------|------|------------|------|------|------------|-----|------|----------------|-----|------|
| | p@3 | p@5 | p@10 | p@3 | p@5 | p@10 | p@3 | p@5 | p@10 | p@3 | p@5 | p@10 |
| Gemini-2.5-pro | 0.43 | 0.43 | 0.43 | 1 | 1 | 1 | 0.33 | 0.4 | 0.1 | 0 | 0 | 0 |
| GPT-4o | 0.32 | 0.32 | 0.32 | 0.21 | 0.21 | 0.21 | 0 | 0.2 | 0.1 | 0.33 | 0.6 | 0.3 |
| Claude-3.7-sonnet | 1 | 1 | 1 | 0.71 | 0.71 | 0.71 | 1 | 1 | 0.9 | 0 | 0 | 0 |
| Grok-3 | 0.69 | 0.69 | 0.69 | 0.89 | 0.89 | 0.89 | 1 | 1 | 1 | 0 | 0 | 0 |
| Doubao-1.5-vision-pro | 0.68 | 0.68 | 0.68 | 0 | 0 | 0 | 0.33 | 0.2 | 0.1 | 0.33 | 0.2 | 0.1 |
| Kimi-VL-A3B | 0 | 0 | 0 | 0 | 0 | 0 | 0 | 0 | 0 | 0 | 0 | 0 |
| Qwen2.5-VL-72B | 0 | 0 | 0 | 0 | 0 | 0 | 0 | 0 | 0 | 0 | 0 | 0 |

Table 21: Per-circuit pass@k scores (k = 3, 5, 10) for CKT13–CKT16 across multiple models

| Model | 17. Oscillator | | | 18. Integrator | | | 19. Differentiator | | | 20. Adder | | |
|-----------------------|----------------|-----|------|----------------|-----|------|--------------------|-----|------|-----------|-----|------|
| | p@3 | p@5 | p@10 | p@3 | p@5 | p@10 | p@3 | p@5 | p@10 | p@3 | p@5 | p@10 |
| Gemini-2.5-pro | 0 | 0 | 0 | 0.33 | 0.4 | 0.1 | 0.2 | 0.1 | 0.33 | 0.4 | 0.1 | 0.33 |
| GPT-4o | 1 | 0.2 | 0.1 | 0.33 | 0.6 | 0.1 | 0.4 | 0.1 | 0 | 0.4 | 0.5 | 0.33 |
| Claude-3.7-sonnet | 0.33 | 1 | 0.3 | 0.33 | 0.2 | 0.1 | 0.33 | 0.2 | 0.1 | 1 | 0.6 | 0.1 |
| Grok-3 | 0.33 | 0.6 | 0.3 | 0.67 | 0 | 0.3 | 0.67 | 0.8 | 0.1 | 0.33 | 0.4 | 0.2 |
| Doubao-1.5-vision-pro | 0.33 | 0.2 | 0.1 | 1 | 0.2 | 0.4 | 0.67 | 0.2 | 0.1 | 0.33 | 0.2 | 0.1 |
| Kimi-VL-A3B | 0 | 0 | 0 | 0 | 0 | 0 | 0 | 0 | 0 | 0 | 0 | 0 |
| Qwen2.5-VL-72B | 0 | 0 | 0 | 0 | 0 | 0 | 0 | 0 | 0 | 0 | 0 | 0 |

Table 22: Per-circuit pass@k scores (k = 3, 5, 10) for CKT17–CKT20 across multiple models

| Model | 21. Subtractor | | | 22. Schmitt trigger | | | 23. VCO | | | 24. Bandgap | | |
|-----------------------|----------------|-----|------|---------------------|------|------|---------|------|------|-------------|-----|------|
| | p@3 | p@5 | p@10 | p@3 | p@5 | p@10 | p@3 | p@5 | p@10 | p@3 | p@5 | p@10 |
| Gemini-2.5-pro | 0.4 | 0.1 | 0.33 | 0.33 | 0.4 | 0.1 | 0.67 | 1 | 0.9 | 0 | 0 | 0 |
| GPT-4o | 0.6 | 0.2 | 0.33 | 0.2 | 0.33 | 0.4 | 0.5 | 0.33 | 0.6 | 0 | 0 | 0 |
| Claude-3.7-sonnet | 1 | 0.8 | 0.2 | 0.33 | 0.4 | 0.1 | 0.33 | 0.2 | 0.2 | 0 | 0 | 0 |
| Grok-3 | 0.33 | 0.2 | 1 | 0.33 | 0.2 | 0.1 | 0.6 | 0.5 | 0.33 | 0 | 0 | 0 |
| Doubao-1.5-vision-pro | 0.33 | 0.2 | 0.1 | 0.33 | 0.2 | 0.1 | 0.67 | 0.2 | 0.1 | 0 | 0 | 0 |
| Kimi-VL-A3B | 0 | 0 | 0 | 0 | 0 | 0 | 0 | 0 | 0 | 0 | 0 | 0 |
| Qwen2.5-VL-72B | 0 | 0 | 0 | 0 | 0 | 0 | 0 | 0 | 0 | 0 | 0 | 0 |

Table 23: Per-circuit pass@k scores (k = 3, 5, 10) for CKT21–CKT24 across multiple models

| Model | 25. Comparator | | | 26. LDO | | | 27. PLL | | | 28. SAR-ADC | | |
|-----------------------|----------------|-----|------|---------|-----|------|---------|-----|------|-------------|-----|------|
| | p@3 | p@5 | p@10 | p@3 | p@5 | p@10 | p@3 | p@5 | p@10 | p@3 | p@5 | p@10 |
| Gemini-2.5-pro | 0 | 0 | 0 | 0 | 0 | 0 | 0 | 0 | 0 | 0 | 0 | 0 |
| GPT-4o | 0 | 0 | 0 | 0 | 0 | 0 | 0 | 0 | 0 | 0 | 0 | 0 |
| Claude-3.7-sonnet | 0 | 0 | 0 | 0 | 0 | 0 | 0 | 0 | 0 | 0 | 0 | 0 |
| Grok-3 | 0 | 0 | 0 | 0 | 0 | 0 | 0 | 0 | 0 | 0 | 0 | 0 |
| Doubao-1.5-vision-pro | 0 | 0 | 0 | 0 | 0 | 0 | 0 | 0 | 0 | 0 | 0 | 0 |
| Kimi-VL-A3B | 0 | 0 | 0 | 0 | 0 | 0 | 0 | 0 | 0 | 0 | 0 | 0 |
| Qwen2.5-VL-72B | 0 | 0 | 0 | 0 | 0 | 0 | 0 | 0 | 0 | 0 | 0 | 0 |

Table 24: Per-circuit pass@k scores (k = 3, 5, 10) for CKT25–CKT28 across multiple models

A.3.2 Testbench Design Task

| ID | Circuit Type | # Metrics | ID | Circuit Type | # Metrics |
|----|--------------------------------------|--|----|--------------------|--|
| 1 | Cross-coupled differential amplifier | CMRR, DC gain, GBW, Phase margin, Power, PSR, SR | 7 | LDO | LDR, LNR, Drop voltage, DC gain, Phase margin, PSR, Offset |
| 2 | Comparator | Delay, Offset | 8 | VCO | Jitter, Phase noise |
| 3 | Bootstrap | ENOB | 9 | Unit capacitor | MC-mismatch |
| 4 | Telescopic cascode OTA | CMRR, DC gain, GBW, Phase margin, Power, PSR, SR | 10 | Folded cascode OTA | DC gain, SR, Phase margin, GBW, Power |
| 5 | PLL | Jitter, Phase noise | 11 | SAR-ADC | ENOB |
| 6 | MOS_Ron | Ron | 12 | Bandgap | BuildingupV, Noise, PSR, TC |

Table 25: Testbench design tasks with metrics to be simulated.

| Models | 1. Cross-coupled differential amplifier | | | | | | | 2. Comparator | | 3. Boot- strap |
|-----------------------|---|---------|-----|-----------------|-------------|-------------|----|---------------|-------------|-------------------|
| | CMRR | DC gain | GBW | Phase margin | Power | PSR | SR | Delay | Offset | ENOB |
| Gemini-2.5-pro | 0 | 0 | 0 | 0 | 0 | 0 | 0 | 0 | 0 | 0 |
| GPT-4o | 0 (1) | 0 | 0 | 0 | 0(4) | 0(2) | 0 | 0(2) | 0(2) | 0 |
| Claude-3.7-sonnet | 0 | 0 | 0 | 0 | 0 | 0 | 0 | 0 | 0 | 0 |
| Grok-3 | 0 | 0 | 0 | 0 | 0 | 0 | 0 | 0 | 0 | 0 |
| Doubao-1.5-vision-pro | 0 | 0 | 0 | 0 | 0 | 0 | 0 | 0 | 0 | 0 |
| Kimi-VL-A3B | 0 | 0 | 0 | 0 | 0 | 0 | 0 | 0 | 0 | 0 |
| Qwen2.5-VL-72B | 0 | 0 | 0 | 0 | 0 | 0 | 0 | 0 | 0 | 0 |

Table 26: Cross-coupled differential amplifier, Comparator, and Bootstrap Circuit Design Performance Across Different Models

| Models | 4. Telescopic cascode OTA | | | | | | | 5. PLL | | 6. MOS_Ron |
|-----------------------|---------------------------|---------|-----|-----------------|-------|-----|----|--------|----------------|---------------|
| | CMRR | DC gain | GBW | Phase margin | Power | PSR | SR | Jitter | Phase noise | Ron |
| Gemini-2.5-pro | 0 | 0 | 0 | 0 | 0 | 0 | 0 | 0 | 0 | 0 |
| GPT-4o | 0 | 0 | 0 | 0 | 0 | 0 | 0 | 0 | 0 | 0 |
| Claude-3.7-sonnet | 0 | 0 | 0 | 0 | 0 | 0 | 0 | 0 | 0 | 0 |
| Grok-3 | 0 | 0 | 0 | 0 | 0 | 0 | 0 | 0 | 0 | 0 |
| Doubao-1.5-vision-pro | 0 | 0 | 0 | 0 | 0 | 0 | 0 | 0 | 0 | 0 |
| Kimi-VL-A3B | 0 | 0 | 0 | 0 | 0 | 0 | 0 | 0 | 0 | 0 |
| Qwen2.5-VL-72B | 0 | 0 | 0 | 0 | 0 | 0 | 0 | 0 | 0 | 0 |

Table 27: Telescopic cascode OTA, PLL, and MOS_Ron Performance Across Different Models

| Models | 7. LDO | | | | | | | 8. VCO | | 9. Unit capacitor |
|-----------------------|--------|-----|--------------|---------|--------------|-----|--------|--------|-------------|-------------------|
| | LDR | LNR | Drop voltage | DC gain | Phase margin | PSR | Offset | Jitter | Phase noise | MC-mismatch |
| Gemini-2.5-pro | 0 | 0 | 0 | 0 | 0 | 0 | 0 | 0 | 0 | 0 |
| GPT-4o | 0 | 0 | 0 | 0 | 0 | 0 | 0 | 0 | 0 | 0(3) |
| Claude-3.7-sonnet | 0 | 0 | 0 | 0 | 0 | 0 | 0 | 0 | 0 | 0 |
| Grok-3 | 0 | 0 | 0 | 0 | 0 | 0 | 0 | 0 | 0 | 0 |
| Doubao-1.5-vision-pro | 0 | 0 | 0 | 0 | 0 | 0 | 0 | 0 | 0 | 0 |
| Kimi-VL-A3B | 0 | 0 | 0 | 0 | 0 | 0 | 0 | 0 | 0 | 0 |
| Qwen2.5-VL-72B | 0 | 0 | 0 | 0 | 0 | 0 | 0 | 0 | 0 | 0 |

Table 28: LDO, VCO, and Unit Capacitor Performance Across Different Models

| Models | 10. Folded cascode OTA | | | | | 11. SAR-ADC | 12. Bandgap | | | |
|-----------------------|------------------------|----|--------------|-----|-------|-------------|-------------|-------------|-----|----|
| | DC gain | SR | Phase margin | GBW | Power | ENOB | BuildiupV | Noise | PSR | TC |
| Gemini-2.5-pro | 0 | 0 | 0 | 0 | 0 | 0 | 0 | 0 | 0 | 0 |
| GPT-4o | 0 | 0 | 0 | 0 | 0 | 0 | 0 | 0(1) | 0 | 0 |
| Claude-3.7-sonnet | 0 | 0 | 0 | 0 | 0 | 0 | 0 | 0 | 0 | 0 |
| Grok-3 | 0 | 0 | 0 | 0 | 0 | 0 | 0 | 0 | 0 | 0 |
| Doubao-1.5-vision-pro | 0 | 0 | 0 | 0 | 0 | 0 | 0 | 0 | 0 | 0 |
| Kimi-VL-A3B | 0 | 0 | 0 | 0 | 0 | 0 | 0 | 0 | 0 | 0 |
| Qwen2.5-VL-72B | 0 | 0 | 0 | 0 | 0 | 0 | 0 | 0 | 0 | 0 |

Table 29: Folded Cascode OTA, SAR-ADC, and Bandgap Performance Across Different Models

B Test Examples

B.1 Examples of perception tasks

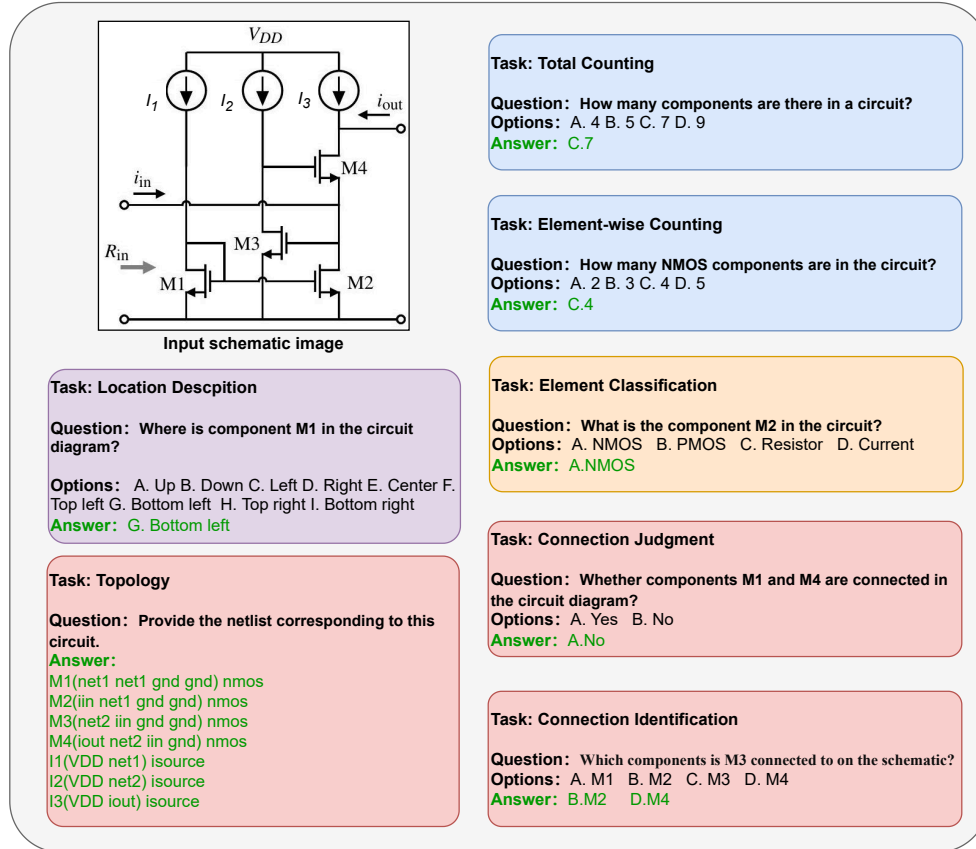
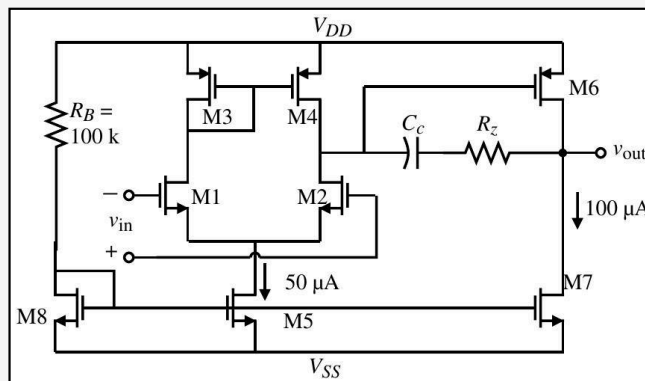


Figure 9: Example of **Perception** task in AMSbench



Question: Could you determine this circuit and the constituent structures it contains?

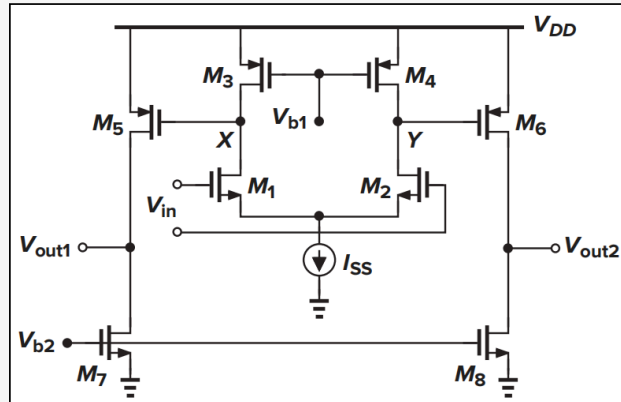
Options:

- | | |
|--|---|
| A. Cascade structure | E. Cascode Structure |
| B. Telescopic Cascode Structure | F. Miller Compensation with Nulling Resistor |
| C. Differential Pair | G. Folded Cascode Structure |
| D. Miller Compensation | H. Simple Current Mirror |

Answer: A, C, F, H

Figure 10: Example of **Partition** task in AMSbench

B.2 Examples of analysis tasks



Question: According to the following circuit diagram, tell me why the circuit represented by this diagram is an operational amplifier?

Options:

A. Through the coordination of the differential input stage, the high-gain intermediate stage and the output stage, high voltage gain and differential signal processing capabilities are achieved, which conforms to the core characteristics of an operational amplifier, namely "high gain, differential input, and signal amplification ability". Therefore, it belongs to the operational amplifier circuit.

B. This circuit does not meet the typical structural requirements of an operational amplifier: An operational amplifier usually consists of an input stage (differential amplification), a high-gain intermediate stage, and an output stage (such as a push-pull structure), and it needs to have characteristics such as high gain and frequency compensation. However, this circuit only exhibits a differential input structure (M1, M2), lacking the crucial intermediate high-gain amplification stage and the standard output stage (such as a push-pull output circuit), and it also does not have components related to frequency compensation. As a result, it cannot achieve the core functions required for an operational amplifier, such as high gain, low output impedance, and stable amplification. Therefore, it does not belong to an operational amplifier circuit.

C. An operational amplifier needs to have a complete frequency compensation mechanism to ensure the stability of the circuit (for example, by implementing phase margin adjustment through a Miller capacitor, etc.). However, this circuit has not designed any structure related to frequency compensation. It cannot effectively suppress self-excited oscillation under different input signal frequencies, nor can it ensure the stability during closed-loop operation. This is a clear deficiency compared to the stable amplification characteristics (including the stability of the frequency response) that an operational amplifier must meet. Therefore, it does not belong to an operational amplifier circuit.

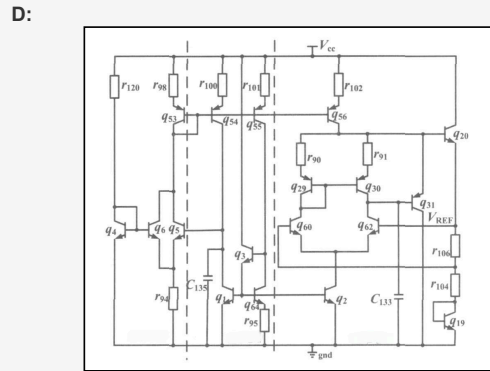
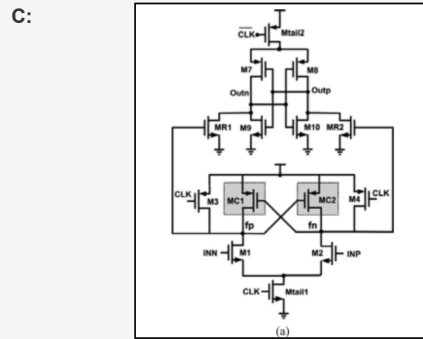
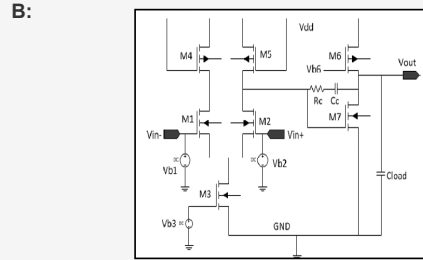
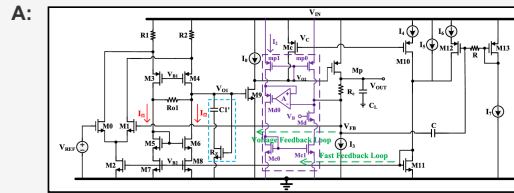
D. The circuit diagram does not represent an operational amplifier because it lacks the key characteristics of an operational amplifier, such as the feedback mechanism, multi-stage amplification, and buffered output structures. Its output stage is simple and cannot achieve the high gain and stable performance required by an operational amplifier.

Answer: A

Figure 11: Examples of **Reasoning** task in AMSbench

Function Image Task

Question: Choose the schematic that represents a comparator.
Options:



GT: C

✦ Gemini-2.5-pro: C (✓)

✖ Grok-3: A (✗)

✦ Qwen2.5-VL-72B: B (✗)

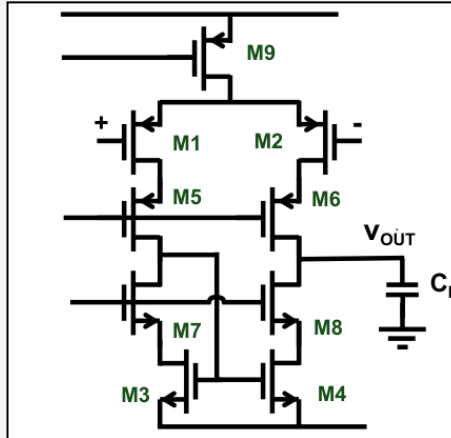
✦ GPT-4o: C (✓)

✦ Claude-3.7-sonnet: B (✗)

✦ Kimi-VL-A3B-Instruct: C (✓)

✦ Doubao-1.5-vision-pro: C (✓)

Figure 12: Example of **Function(image as options)** task in AMSbench



Question: There is a circuit diagram below, please describe this circuit in detail.

Options:

A. In this folded cascode amplifier, cascode transistors M5–M8 are stacked in series with the current mirror and input devices to compensate for the low intrinsic gain of nanometer MOSFETs. The feedback loop around transistor M2 includes cascode M8, which extends the output swing by regulating the drain voltage of M2. The telescopic topology increases output impedance, thereby improving gain without affecting GBW. However, the cascode configuration necessitates a higher supply voltage to maintain proper biasing, resulting in a marginal rise in overall power dissipation..

B. The gain of this voltage amplifier is constrained by the low intrinsic gain of cascode transistors in nanometer MOSFETs. To enhance performance, four cascode devices (M5–M8) are placed in parallel with the input pair and current mirror. Cascode M5 is integrated into the feedback loop around transistor M1, which stabilizes the gain while maximizing output swing. This telescopic configuration significantly boosts both the output impedance and the gain-bandwidth product (GBW) due to improved loop gain, though the additional cascode stages introduce a slight increase in power consumption from elevated bias currents.

C. The gain of such a voltage amplifier is rather limited as the gain per transistor can be quite small for nanometer MOS devices. This is why cascodes are better added. Four cascode MOS transistors are added M5–8 in series with the input devices and current mirror, as shown in this slide. Note that cascode M7 is included in the feedback loop around transistor M3, which allows a larger output swing. This is called the telescopic CMOS OTA. The impedance at the output node increases considerably, but not the GBW.

D. This telescopic CMOS OTA addresses limited per-stage gain by incorporating cascode transistors M5–M8 in series with the differential input pair. Cascode M6 is embedded within the feedback loop surrounding transistor M4, enabling wider output swing and higher DC gain. The elevated output impedance directly enhances the GBW, as the cascodes reduce parasitic capacitance at the output node. Despite the added complexity, power consumption remains unchanged because the cascode devices operate in the saturation region without altering the bias current.

GT: A

Figure 14: Example of **Caption** task in AMSbench

B.3 Examples of design tasks

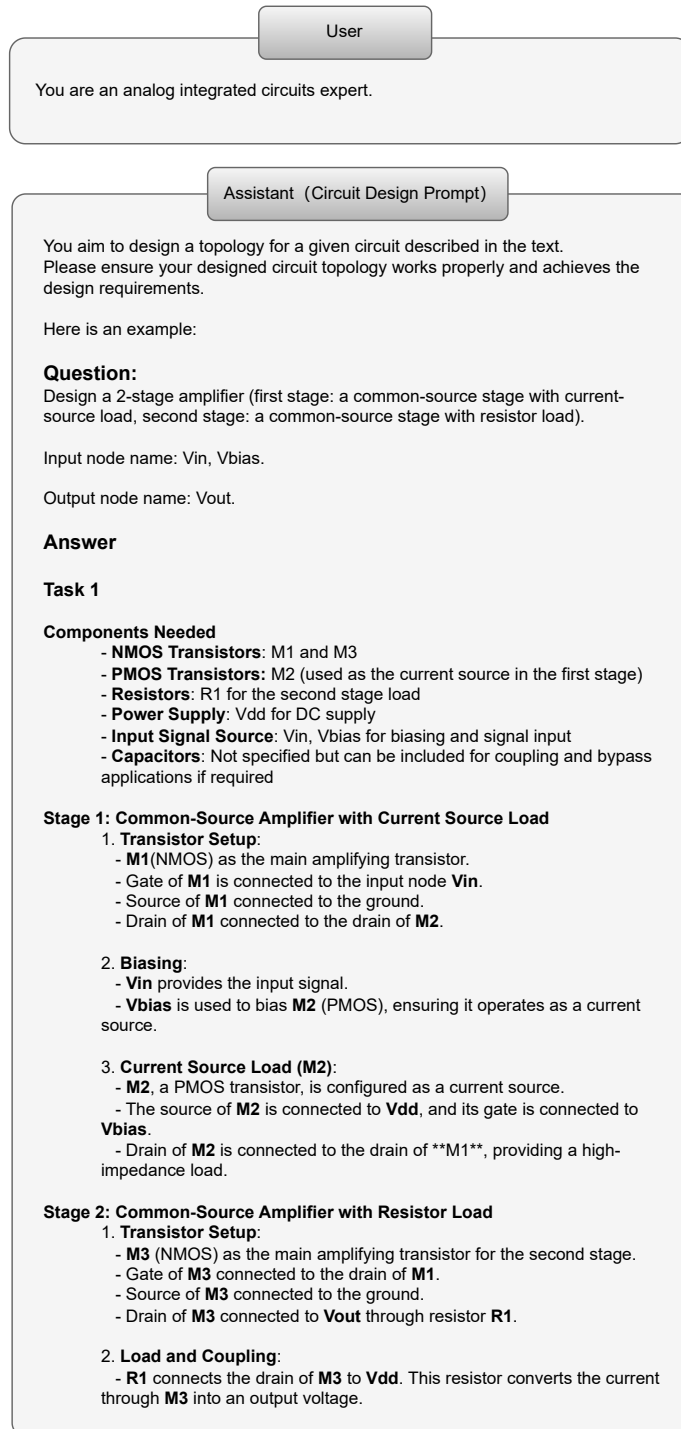


Figure 15: Prompt of **Circuit Design** task in AMSbench

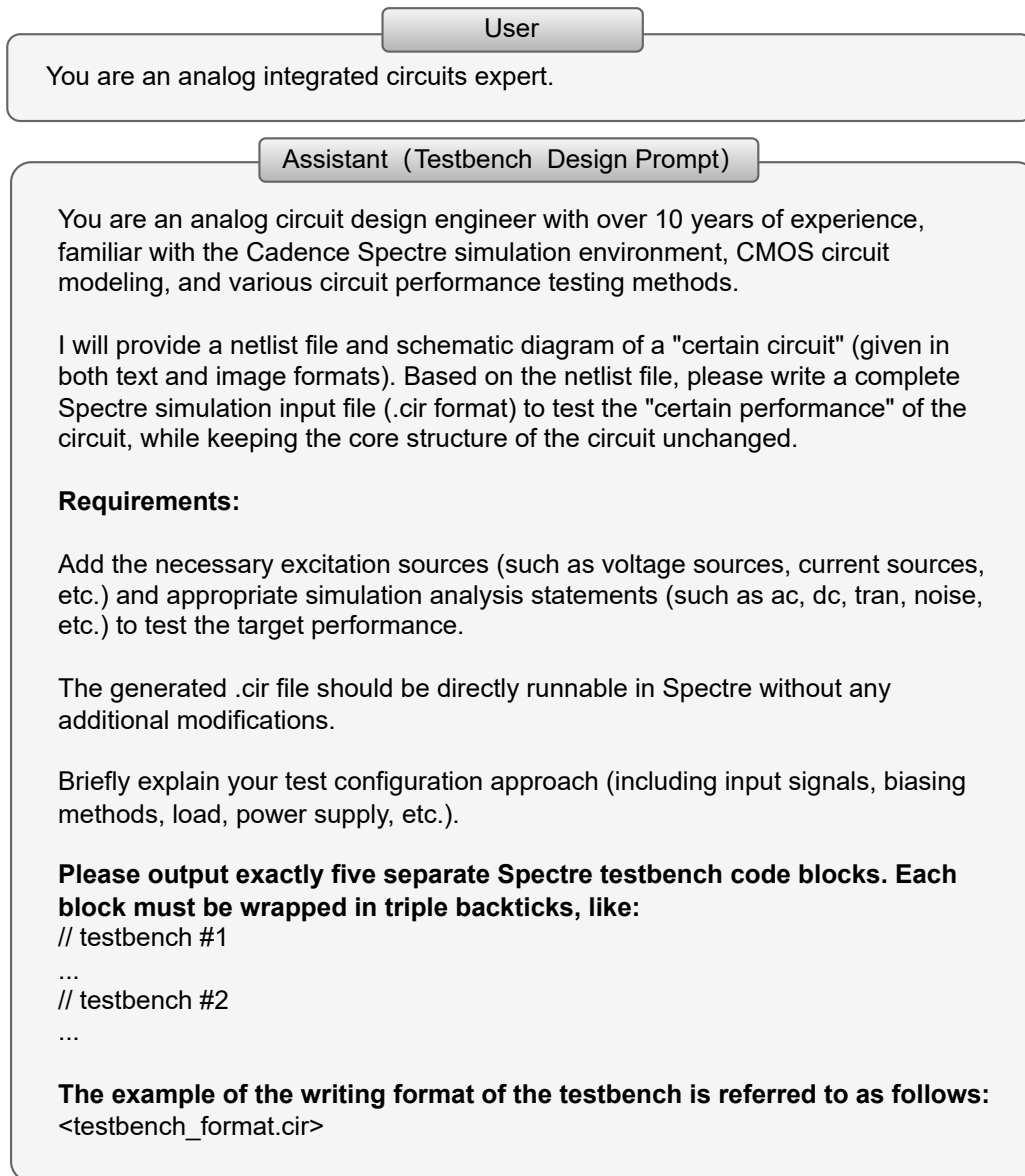


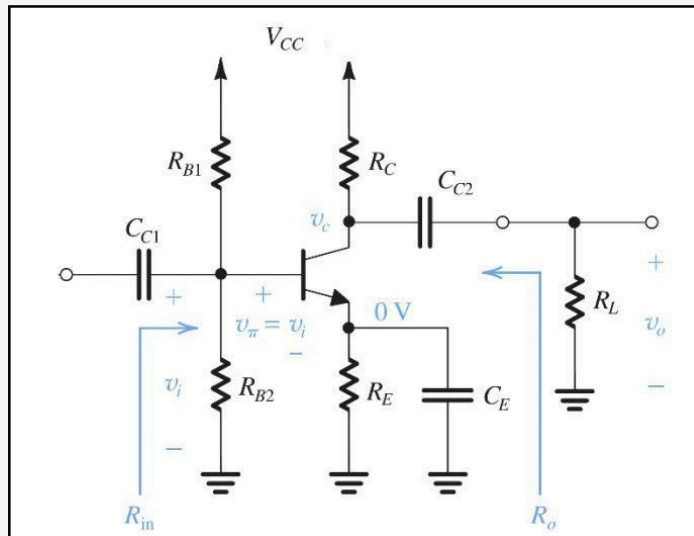
Figure 16: Prompt of **Testbench Design** task in AMSbench

C Case Study

C.1 Perception task for Error Analysis

Total Counting Task

Test Image:



Question: How many components are there in a circuit?

GT: 9



Gemini-2.5-pro: 9 (✓)



Grok-3: 9 (✓)



Qwen2.5-VL-72B: 6 (✗)



GPT-4o: 9 (✓)



Claude-3.7-sonnet: 8 (✗)



Kimi-VL-A3B-Instruct: 10 (✗)

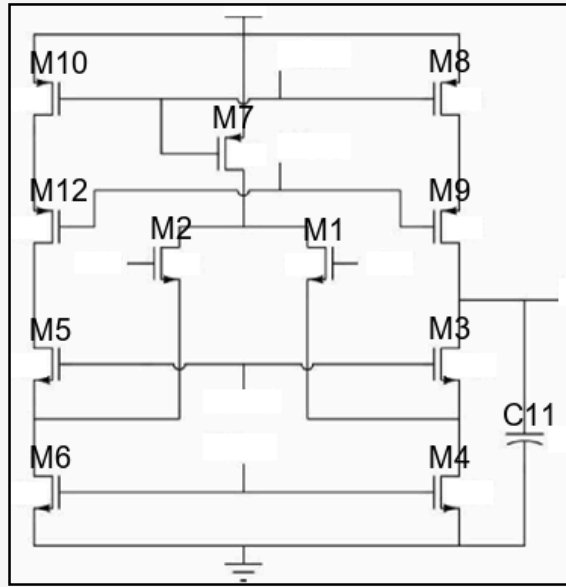


Doubao-1.5-vision-pro: 8 (✗)

Figure 17: Example of **Total Counting** task across models

Type-wise Counting Task

Test Image:



Question: How many PMOS components are in the circuit?

GT: 5



Gemini-2.5-pro: 5 (✓)



Grok-3: 3 (✗)



Qwen2.5-VL-72B: 6 (✗)



GPT-4o: 5 (✓)



Claude-3.7-sonnet: 6 (✗)



Kimi-VL-A3B-Instruct: 8 (✗)

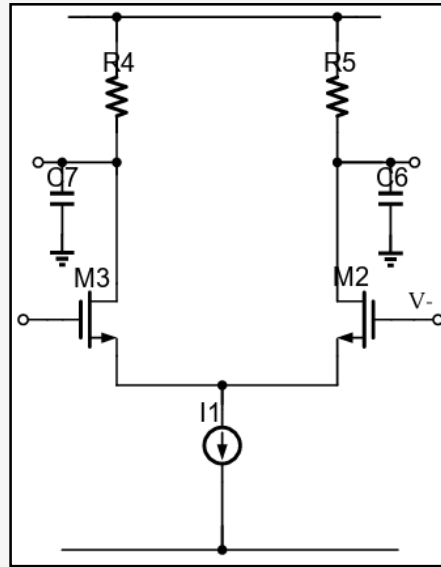


Doubao-1.5-vision-pro: 6 (✗)

Figure 18: Example of **Type-wise Counting** task across models

Element Classification Task

Test Image:



Question: What is the component M2 in the circuit?

Options:

- A: "current",
- B: "single-end-amp",
- C: "pmos",
- D: "nmos"

GT: D



Gemini-2.5-pro: D (✓)



Grok-3: D (✓)



Qwen2.5-VL-72B: D (✓)



GPT-4o: C (✗)



Claude-3.7-sonnet: D (✓)



Kimi-VL-A3B-Instruct: D (✓)

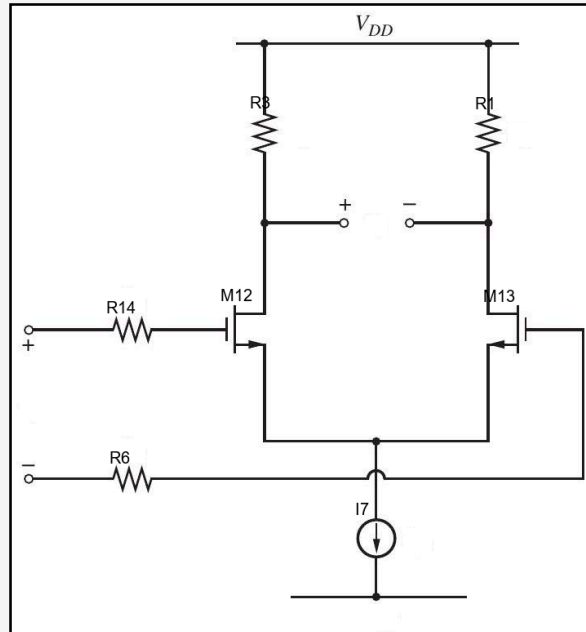


Doubao-1.5-vision-pro: C (✗)

Figure 19: Example of **Element Classification** task across models

Connection Judgment Task

Test Image:



Question: Is M12 connected to R6?

Options:

A: "Yes",

B: "No"

GT: B



Gemini-2.5-pro: A (✗)



Grok-3: A (✗)



Qwen2.5-VL-72B: B (✓)



GPT-4o: B (✓)



Claude-3.7-sonnet: B (✓)



Kimi-VL-A3B-Instruct: A (✗)

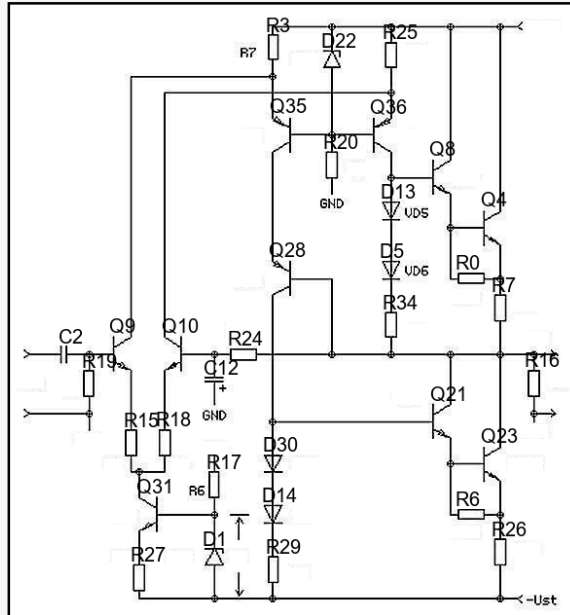


Doubao-1.5-vision-pro: A (✗)

Figure 20: Example of **Connection Judgment** task across models

Connection Identification Task

Test Image:



Question: Which components is R15 connected to?

Options:

- | | |
|-----------|-----------|
| A: "Q9", | B: "R3", |
| C: "C2", | D: "Q28", |
| E: "Q31", | F: "R17", |
| G: "R18", | H: "R15" |

GT: A,E,G



Gemini-2.5-pro: A,E,G (✓)



Grok-3: A,G (✗)



Qwen2.5-VL-72B: G (✗)



GPT-4o: B,F,G (✗)



Claude-3.7-sonnet: A,E,G (✓)



Kimi-VL-A3B-Instruct:
A,D,E,F,G,H (✗)

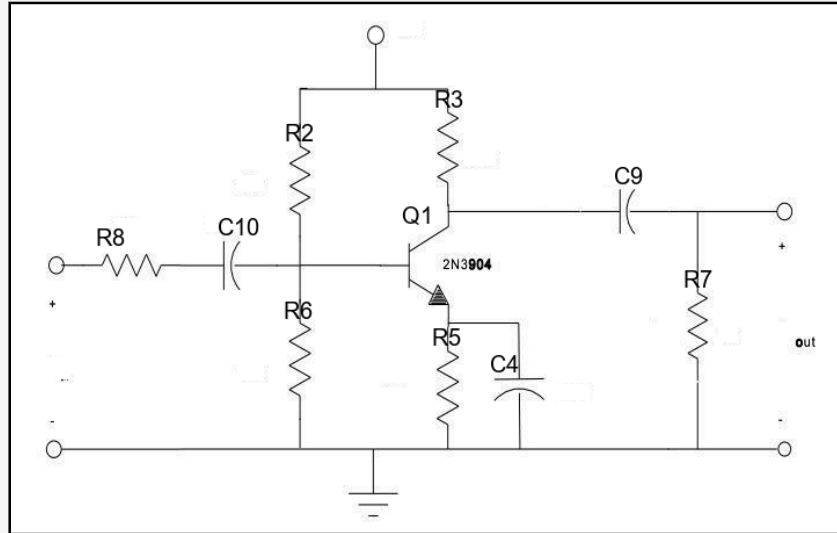


Doubao-1.5-vision-pro: A,E,G (✓)

Figure 21: Example of **Connection Identification** task across models

Location Description Task

Test Image:



Question: What part of the circuit does the C4 occupy?

Options:

- | | |
|-------------------|--------------|
| A: "Bottom", | B: "Center", |
| C: "Bottom left", | D: "Right", |
| E: "Top right", | F: "Left", |
| G: "Top left", | H: "Top", |
| I: "Bottom right" | |

GT: A

✦ Gemini-2.5-pro: I (✗)

✧ Grok-3: A (✓)

✦ Qwen2.5-VL-72B: A (✓)

✧ GPT-4o: C (✗)

✦ Claude-3.7-sonnet: I (✗)

✧ Kimi-VL-A3B-Instruct:B (✗)

✦ Doubao-1.5-vision-pro: C (✗)

Figure 22: Example of **Location Description** task across models

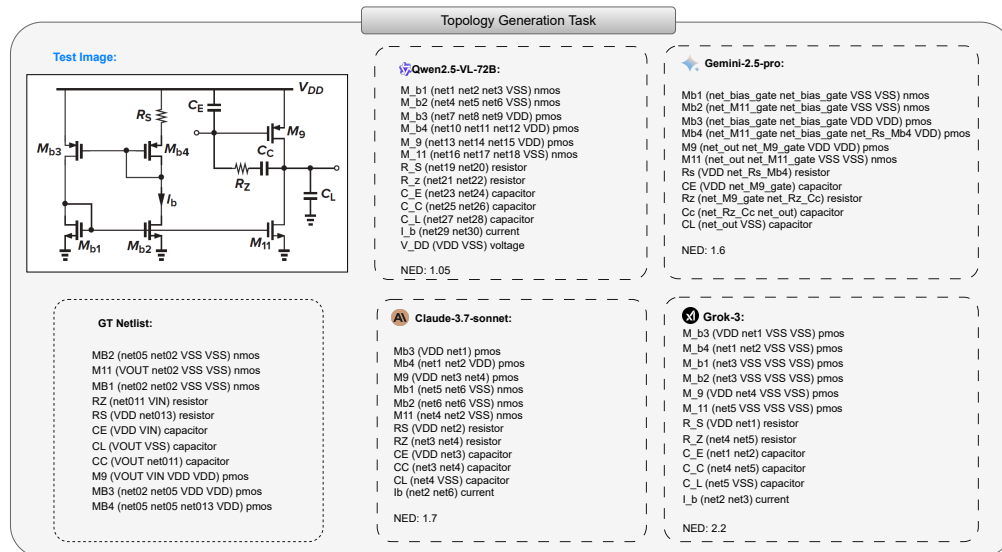
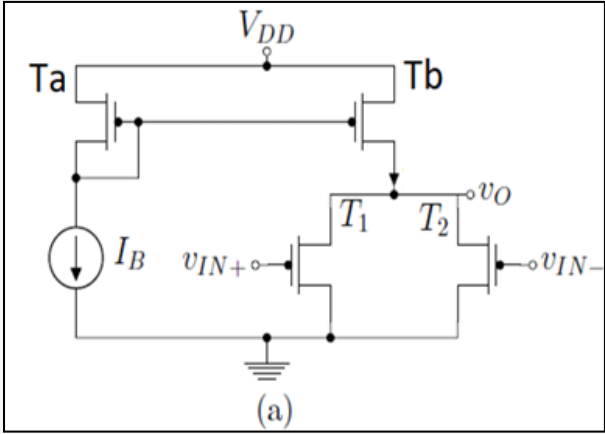


Figure 23: Example of **Topology Generation** task across models

C.2 Analysis task for Error Analysis

Function Text Task

Test Image:





Question: What is the circuit's primary functional type in the diagram?


Options:


- A: "LDO",
- B: "Op-amp",
- C: "Comparator",
- D: "Bandgap"


GT: B


 Gemini-2.5-pro: B (✓)

 Grok-3: B (✓)

 Qwen2.5-VL-72B: B (✓)

 GPT-4o: C (✗)

 Claude-3.7-sonnet: C (✗)

 Kimi-VL-A3B-Instruct: C (✗)


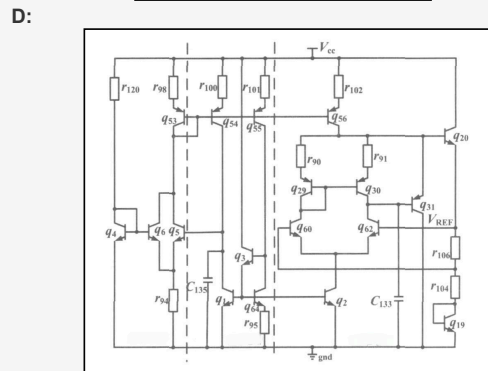
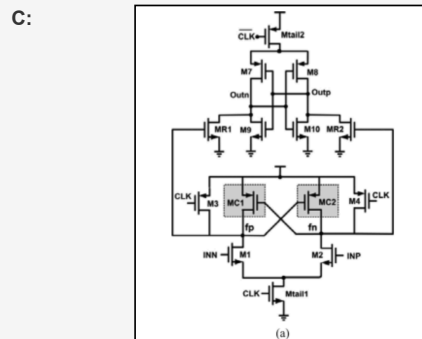
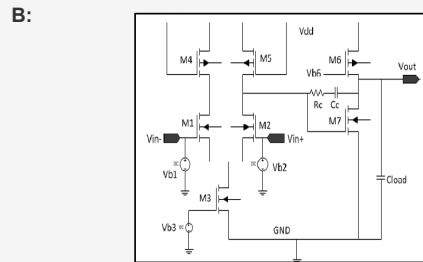
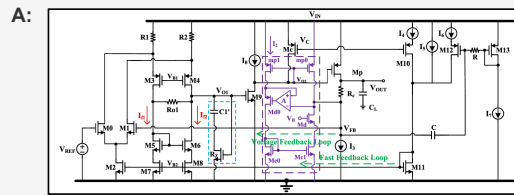
 Doubao-1.5-vision-pro: B (✓)

Figure 24: Example of **Function Text** task across models

Function Image Task

Question: Choose the schematic that represents a comparator.
Options:



GT: C

✦ Gemini-2.5-pro: C (✓)

✖ Grok-3: A (✗)

✦ Qwen2.5-VL-72B: B (✗)

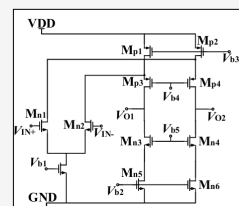
✦ GPT-4o: C (✓)

✦ Claude-3.7-sonnet: B (✗)

✦ Kimi-VL-A3B-Instruct: C (✓)

✦ Doubao-1.5-vision-pro: C (✓)

Figure 25: Example of **Function Image** task across models



GT: This circuit qualifies as an operational amplifier because the circuit includes a differential input stage formed by transistors M1 and M2, which is a fundamental feature of any operational amplifier. These transistors receive differential signals at their gates (VIN+ and VIN-), enabling differential signal amplification. Tail current sources are implemented using transistors M3 and M2, which help to set a proper operating point for M3-M4. The transistors M5 and M6 form a common-emitter stage, which provides the bias voltage Vb2 and Vb5, which can increase output impedance. A gain stage is built with transistors M3, M4, which function as a cascode and further amplify the signal. The outputs VO1 and VO2 suggest a differential output configuration, which is common in full op-amp designs. Multiple bias voltages (Vb1, Vb2, Vb3, Vb4, and Vb5) are used to properly bias the various stages of the circuit, which is a typical approach in analog integrated op-amp design to maintain correct operating points.

The circuit is an operational amplifier primarily due to its differential pair M_1 and M_2 , which amplify the input voltage difference through a **resistive load** formed by M_3 and M_4 . A current source at the tail of the input stage, implemented by M_5 and M_6 under V_{b2} control, sets the quiescent current. The cascode stage M_1 and M_2 provides voltage gain by stacking transistors, while M_5 and M_6 serve as active loads for the output stage, producing the differential outputs V_{O1} and V_{O2} . The bias voltages (V_{b1} – V_{b5}) are critical for adjusting the transconductance of the input stage and tuning the cascode's gain, which aligns with conventional op-amp architectures that prioritize high open-loop gain and differential signal processing. (x)

This circuit qualifies as an differential input stage because the input signals are sensed by two gates formed by transistors M1 and M2, which is a fundamental feature of any operational amplifier. These transistors receive differential signals at their gates (V_{IN+} and V_{IN-}), enabling differential signal amplification. Tail current sources are implemented using transistors M1 and M2, which help to set a proper operating point for M3-Mp4. The transistors M3 and M4 are connected in series, forming a cascode by the bias voltage Vb2 and Vb5, which can increase output impedance. A gain stage is built with transistors M3, Mp4, which function as a cascode and further amplify the signal. The outputs V01 and V02 suggest a differential output configuration, which is common in full differential op-amp designs. Multiple bias voltages (Vb1, Vb2, Vb3, Vb4, and Vb5) are used to properly bias various stages of the circuit, ensuring optimal performance and stability. The op-amp design is implemented using correct operating points. (3)

This circuit qualifies as an operational amplifier because: The circuit includes a differential input stage formed by transistors M1 and M2, which is a fundamental feature of any operational amplifier. These transistors receive differential signals at their gates (V_{IN+} and V_{IN-}), enabling differential signal amplification. Tail current sources are implemented using transistors M1 and M2, which help to set a proper operating point for Mp3-Mp4. The transistors Mp3 and Mp4 are configured as a common-emitter stage, where the bias voltage Vb2 and Vb5, which can increase output impedance. A gain stage is built with transistors Mp3, Mp4, which function as a cascode and further amplify the signal. The outputs V01 and V02 suggest a differential output configuration, which is common in full differential op-amp designs. Multiple bias voltages (Vb1, Vb2, Vb3, Vb4, and Vb5) are used, indicating a complex biasing scheme, which is a typical approach in analog integrated op-amp design to maintain correct operating points. (✓)

The circuit is an operational amplifier primarily due to its differential pair Mn1 and Mn2, which amplify the input voltage difference through a **resistive load formed by Mp3 and Mp4**. A current source at the tail of the input stage, **implemented by Mn5 and Mn6 under Vb2 control**, sets the quiescent current. The cascode stage **Mn1 and Mn2** provides voltage gain by stacking transistors, while **Mp5 and Mp6** serve as active loads for the output stage, producing the differential outputs V01 and V02. The bias voltages (Vb1–Vb5) are critical for adjusting the transconductance of the input stage and tuning the cascode's gain, which aligns with conventional op-amp architectures that prioritize high open-loop gain and differential signal processing. (x)

This circuit qualifies as an operational amplifier because:
The circuit includes a differential input stage formed by transistors Mm1 and Mm2, which is a fundamental feature of any operational amplifier. These transistors receive differential signals at their gates (V_{IN+} and V_{IN-}), enabling differential signal amplification. Tail current sources are implemented using transistors Mp1 and Mp2, which help to set the operating point and provide a common-mode feedback path.
The output stage consists of a cascode configuration of transistors Mm3-Mm6 forming a cascode current source, indicated by the bias voltage Vb2 and Vb5, which can increase output impedance. A gain stage is built with transistors Mp3, Mp4, which function as a cascode and further amplify the signal. The outputs VOUT1 and VOUT2 suggest a differential output configuration, which is common in fully differential op-amp designs. Multiple bias voltages (Vb1, Vb2, Vb3, Vb4, and Vb5) are used, indicating a complex biasing scheme, which is a typical approach in analog integrated op-amp design to maintain correct operating points. (✓)

This circuit qualifies as an operational amplifier because: The circuit includes a differential input stage formed by transistors $Mn1$ and $Mn2$, which is a fundamental feature of any operational amplifier. These transistors receive differential signals at their gates (V_{IN+} and V_{IN-}), enabling differential signal amplification. Tail current sources are implemented using transistors $Mp1$ and $Mp2$, which help to set a proper operating point for $Mp3$ - $Mp4$. The transistors $Mn3$ and $Mn4$ form a cascode stage, which increases the bias voltage $Vb2$ and $Vb5$, which can increase output impedance. A gain stage is built with transistors $Mp3$, $Mp4$, which function as a cascode and further amplify the signal. The outputs V_{O1} and V_{O2} suggest a differential output configuration, which is common in fully differential op-amp designs. Multiple bias voltages ($Vb1$, $Vb2$, $Vb3$, $Vb4$, and $Vb5$) are used to properly bias the circuit, which is a typical approach in analog integrated-circuit design to maintain correct operating points. (3)

The circuit is an operational amplifier primarily due to its differential pair Mn1 and Mn2, which amplify the input voltage difference through a **resistive load formed by Mp3 and Mp4**. A current source at the tail of the input stage, **implemented by Mn5 and Mn6 under Vb2 control**, sets the quiescent current. The cascode stage **Mp1 and Mp2** provides voltage gain by stacking transistors, while **Mp5 and Mp6** serve as active loads for the output stage, producing the differential outputs VO1 and VO2. The bias voltages (Vb1–Vb5) are critical for adjusting the transconductance of the input stage and tuning the cascode's gain, which aligns with conventional op-amp architectures that prioritize high open-loop gain and differential signal processing. (x)

39

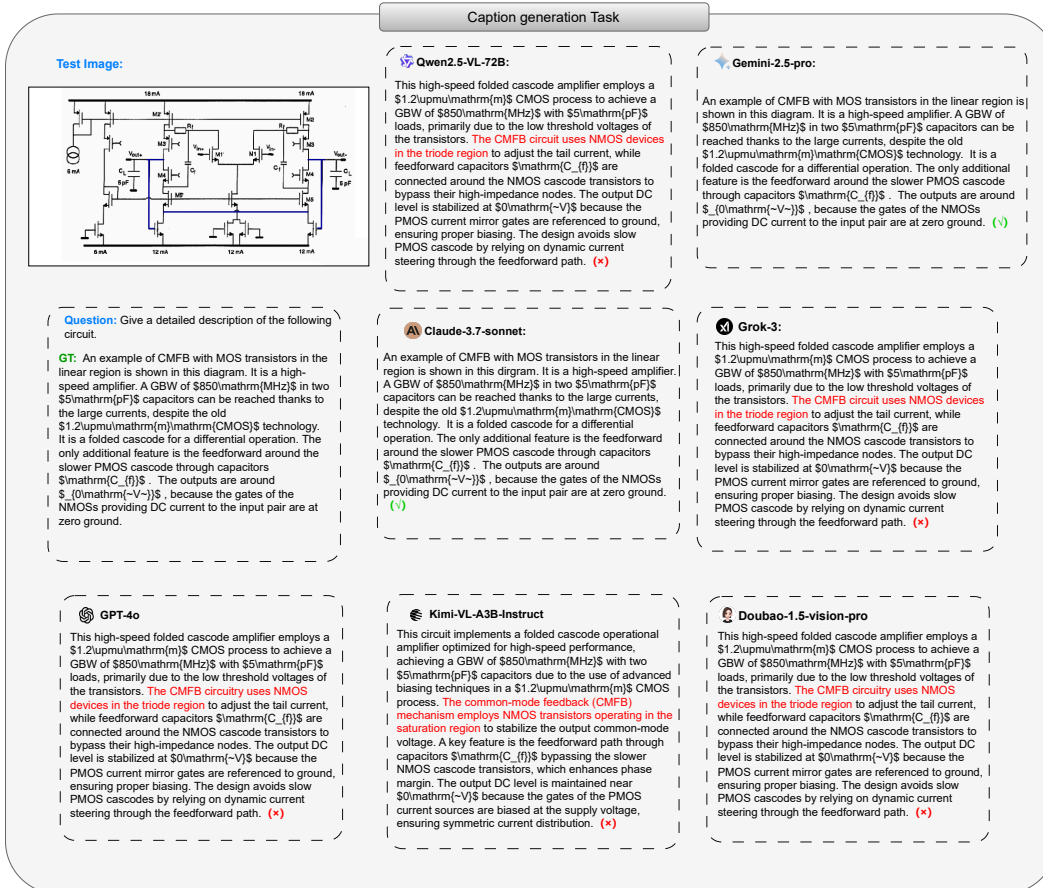


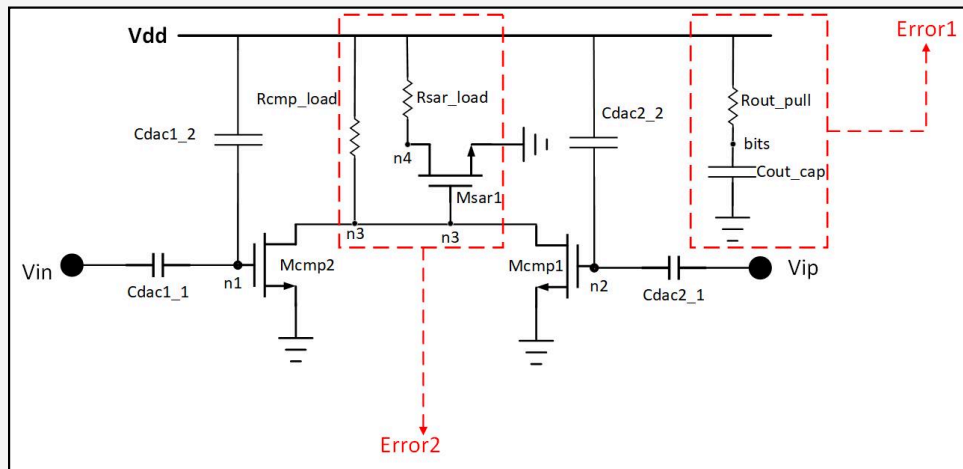
Figure 28: Example of Caption Generation task across models

C.3 Design task for Error Analysis

Error netlist example of SAR-ADC design by GPT-4o

Netlist generated by GPT4o:

```
Vdd Vdd 0 5.0
Vin Vin 0 2.5
Vip Vip 0 2.7
Cdac1_1 Vin n1 1pF
Cdac1_2 n1 Vdd 1pF
Cdac2_1 Vip n2 1pF
Cdac2_2 n2 Vdd 1pF
Mcmp1 n3 n2 gnd gnd nmos_model l=1e-06 w=5e-05
Mcmp2 n3 n1 gnd gnd nmos_model l=1e-06 w=5e-05
Rcmp_load n3 Vdd 10kOhm
Msar1 n4 n3 gnd gnd nmos_model l=1e-06 w=5e-05
Rsar_load n4 Vdd 10kOhm
Rout_pull bits Vdd 10kOhm
Cout_cap bits gnd 1pF
.model nmos_model nmos (kp=0.0001 level=1 vto=0.5)
.model pmos_model pmos (kp=5e-05 level=1 vto=-0.5)
```



Schematic

Figure 29: Example of **Circuit Design** task by GPT-4o

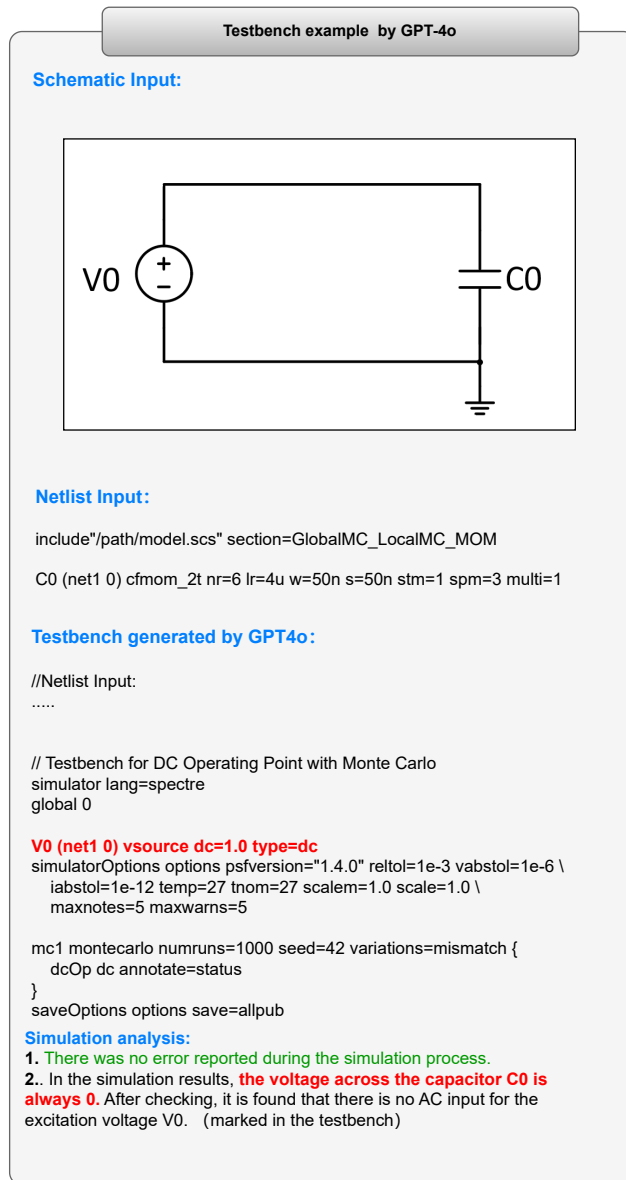


Figure 30: Example of **Testbench Design** task by GPT-4o